Executable models of pathways built using single-cell RNA seq data reveal immune signaling dysregulations in people living with HIV and atherosclerosis

Mukta G. Palshikar[1], Rohith Palli[2], Alicia Tyrell[3], Sanjay Maggirwar[4], Giovanni Schifitto[5, 6], Meera V. Singh[5, 8,] and Juilee Thakar[1, 7, 8, 9**]

**Correspondence: Juilee_Thakar@URMC.Rochester.edu

[1] Biophysics, Structural, and Computational Biology Program, University of Rochester School of Medicine and Dentistry, Rochester, USA. [6] Department of Biostatistics and Computational Biology, University of Rochester School of Medicine and Dentistry, Rochester, USA. [7] Department of Microbiology and Immunology, University of Rochester School of Medicine and Dentistry, Rochester, USA. [8] Department of Biomedical Genetics, University of Rochester School of Medicine and Dentistry, Rochester, USA

Full list of author information is available at the end of the article

Abstract:

Background: Atherosclerosis (AS)-associated cardiovascular disease is an important cause of mortality in an aging population of people living with HIV (PLWH). This elevated risk of atherosclerosis has been attributed to viral infection, prolonged usage of anti-retroviral therapy, and subsequent chronic inflammation.

Methods: To investigate dysregulated immune signaling in PLWH with and without AS, we sequenced 9368 peripheral blood mononuclear cells (PBMCs) from 8 PLWH, 4 of whom also had atherosclerosis (AS+). To develop executable models of signaling pathways that drive cellular states in HIV-associated atherosclerosis, we developed the single-cell Boolean Omics Network Invariant Time Analysis

(scBONITA) algorithm. ScBONITA (a) uses single-cell RNA sequencing data to infer Boolean rules for topologically characterized networks, (b) prioritizes genes based on their impact on signaling, (c) performs pathway analysis, and (d) maps sequenced cells to characteristic signaling states. We used scBONITA to identify dysregulated pathways in different cell-types from AS+ PLWH and AS- PLWH. To compare our findings with pathways associated with HIV infection, we used scBONITA to analyze a publicly available dataset of PBMCs from subjects before and after HIV infection. Additionally, the executable Boolean models characterized by scBONITA were used to analyze observed cellular states corresponding to the steady states of signaling pathways

Results: We identified an increased subpopulation of CD8+ T cells and a decreased subpopulation of monocytes in AS+ PLWH. Dynamic modeling of signaling pathways and pathway analysis with scBONITA provided a new perspective on the mechanisms of HIV-associated atherosclerosis. Lipid metabolism and cell migration pathways are induced by AS rather than by HIV infection. These pathways included AGE-RAGE and PI3K-AKT signaling in CD8+ T cells, and glucagon and cAMP signaling pathways in monocytes. Further analysis of other cell subpopulations suggests that the highly interconnected PI3K-AKT signaling pathway drives cell migratory state in response to dyslipidemia. scBONITA attractor analysis mapped cells to pathway-specific signaling states that correspond to distinct cellular states.

Conclusions: Dynamic network modeling and pathway analysis with scBONITA indicates that dysregulated lipid signaling regulates cell migration into the vascular endothelium in AS+ PLWH. Attractor analysis with scBONITA facilitated pathway-based characterization of cellular states that are not apparent in gene expression analyses.

Keywords: single-cell RNA sequencing; Boolean networks; HIV; atherosclerosis; pathway analysis; network modeling

Background

Human immunodeficiency virus (HIV) infection greatly increases the risk of atherosclerosis (AS) associated cardiovascular disease (CVD), which is a leading cause of morbidity and mortality in persons living with HIV (PLWH) (1-4). Several factors contribute to this elevated risk of AS. PLWH have a higher prevalence of traditional risk factors for AS such as dyslipidemia, diabetes, hypertension, and smoking (5-9). In addition, the off-target effects of certain classes of antiretroviral drugs lead to an increase in traditional metabolic risk factors such as dyslipidemia, weight gain, and metabolic syndrome (9, 10). However, PLWH have an elevated risk of developing CVD even when controlling for these risk factors (4, 11, 12). Finally, HIV infection itself causes metabolic changes leading to a pro-atherogenic inflammatory environment in the vasculature (13-16).

HIV infection and long-term antiretroviral therapy modulate signaling dynamics, leading to changes in the composition of peripheral blood mononuclear cells (PBMCs) and in the expression of functionally important molecules in these cells (17). HIV infection mediates an array of molecular signaling pathways, including inflammasome activation, cell migration and apoptosis. These signaling pathways contribute to immune cell activation and inflammation in the vasculature (18). Biomarker studies also highlight the importance of these processes in atherogenesis, especially in the context of activated monocyte/macrophages and T cells (14-16). CD8+ T cells contribute to the atherogenic environment by cytokine secretion, secretion of cytotoxic granules and formation of the necrotic core of atherosclerotic plaques (reviewed in (19)). Monocyte/macrophages migrate into the intima and eventually form apoptotic, atherosclerotic plaques (reviewed in (20)). The interplay between immune signaling pathways and immune cell activation and inflammation in the context of HIV infection still requires further investigation. Single-cell measurements of expression profiles allow the investigation of these perturbations simultaneously. To investigate the mechanistic link between HIV infection and atherosclerosis, we used the 10X Genomics platform to sequence ~10,000 PBMCs from 8 PLWH, 4 of whom have atherosclerosis.

Typically, analysis of single cell RNA sequencing (scRNA-seq) data uses clustering methods to define cell subpopulations, followed by differential expression and gene set overrepresentation analysis (ORA) to estimate modulation of molecular pathways in the condition under study. This standard analysis approach discounts pathway topology and falls short of connecting molecular state to cellular state. Furthermore, ORA ignores synergistic interactions among genes by, in effect, treating genes as independent and equal, resulting in a failure to correctly estimate the significance of pathways (21).

Discrete-state network modeling facilitates prioritization of experiments by using simple logic rules such as 'AND' or 'OR' to explicitly define signal integration, enabling investigation of crosstalk and downstream events as shown in our previous studies. Previously, we have extensively used discrete-state network modeling to investigate virus infections and have experimentally validated the predictions (22, 23). We have also developed an algorithm to perform Boolean rule inference and pathway analysis using bulk transcriptomic data. This algorithm has been rigorously tested and compared across other widely used gene-set enrichment methods (24). Here, we expand our discrete-state modeling method and present single-cell Boolean Omics Network Invariant-Time Analysis (scBONITA) to (a) infer Boolean rules (e.g., "AND", "OR") describing signal integration for gene interactions described by the pathway topologies from scRNA-seq data and (b) use these inferred regulatory rules to identify condition-specific dysregulated pathways and to prioritize genes/proteins for further investigation. Instead of simply returning a list of dysregulated pathways and associated p-values, scBONITA returns precise modes of dysregulation, captured by node-level impact scores that quantify the contribution of each node (a gene or protein) to the overall dysregulation of a pathway, measured by *in silico* perturbation and simulation that matches experimental conditions. *In silico* simulation and perturbation of molecular pathways allows the use of scBONITA as a powerful hypothesis-generating tool.

We demonstrate that scBONITA can infer dysregulated pathways from single-cell RNA sequencing (scRNA-seq) data upon HIV infection using publicly available data and in the context of HIV-associated atherosclerosis using data presented in this work. scBONITA identifies dysregulated cell migration and

lipid metabolism related pathways such as PI3K signaling, leukocyte transendothelial migration, and AGE-RAGE signaling in the subpopulations of CD8+ T cells and monocytes, known to be implicated in HIV-associated atherosclerosis. ScBONITA identifies genes, such as the PI3K and PLC genes, which have high impacts on signal flow through the signaling pathways named above. CD4+ T cells and B cells are also known to play significant roles in the development of atherosclerosis and cardiovascular disease (25-35). In both subpopulations, scBONITA identified pathways that were linked to cell migration (such as proteoglycans in cancer and the regulation of actin cytoskeleton pathways), lipid metabolism (P13K-Akt signaling, phosphatidylinositol signaling) and pathways linked to intercellular communication (such as the chemokine signaling, apelin signaling, and cytokine-cytokine receptor interaction pathways).

Furthermore, we used a publicly available dataset of PBMCs from persons before and after HIV infection to show that cell migration pathways are also dysregulated in the early stages of HIV infection, indicating a role for these pathways in both the antiviral response and in subsequent AS (36). We also present a novel method for mapping cells to pathway-specific signaling states using rules identified by BONITA. In conclusion, scBONITA is a powerful tool that can be used for network modeling using single-cell RNA-seq data. In this study, we demonstrate that scBONITA provides an insight into the mechanisms of HIV-associated atherosclerosis at the single-cell level.

Methods

Participant cohort summary, sample collection, and storage

Eight men living with HIV and >= 50 years of age on stable combined antiretroviral therapy (cART) for at least 1 year and with viral load <= 50 copies/mL were recruited. All methods were carried out in accordance with University of Rochester guidelines and regulations, and all experimental and study protocols were approved by the University of Rochester Institutional Review Board (#RSRB00063845). Informed consent was obtained from all subjects. Individuals were classified as having atherosclerosis

(AS+) if they had plaques on the carotid arteries on ultrasound imaging. Four of the 8 subjects were assigned as AS+ and had plaques in both right and left carotid arteries. AS- subjects were aged between 47 and 57 and AS+ subjects were aged between 51 and 66. AS+ subjects had mean serum cholesterol of 161.5 mg/dl (σ = 40.9) and mean serum high-density lipid HDL of 54.7 mg/dl (σ = 16.3). AS- subjects had mean serum cholesterol of 167.7 mg/dl (σ =57.2) and mean serum high-density lipid HDL of 51 mg/dl (σ = 7.7). AS- subjects and AS+ subjects had a mean CD4+ T cell count of 518.5 cells/µl (σ =347.8 cells/µl) and 838.7 cells/µl (σ = 514.5 cells/µl) respectively. 30 mls of blood per study participant was collected in ACD vacutainers and was processed within 2 - 3 hours of collection. Peripheral Blood Mononuclear Cells (PBMCs) were isolated using Ficoll density gradient centrifugation. 5 million PBMCs were preserved using RNAlater (Thermo Fisher) and were used for scRNA-seq. De-identified subject information is available in Supplementary File 1, Supplementary Figure 1.

Single-cell sequencing and data processing

Frozen vials containing cells in RNAlater were thawed quickly in a 37-degree water bath. Cell suspension was transferred to a 15ml conical tube. 10 ml PBS/2% FBS was slowly added. Samples were centrifuged at 1600rpm for 6 min. Washes were repeated for an additional 2 times for a total of 3 washes. Using the MACS Miltenyi Biotec Dead Cell removal kit (PN130-090-101), dead cells were removed using manufacturer's recommendations. Cells were counted and cellular suspensions were loaded on a Chromium Single-Cell Instrument (10x Genomics, Pleasanton, CA, USA) to generate single-cell Gel Bead-in-Emulsions (GEMs). ScRNA-seq libraries were prepared using Chromium Single-Cell 3' Library & Gel Bead Kit (10x Genomics). The beads were dissolved, and cells were lysed per manufacturer's recommendations. GEM reverse transcription (GEM-RT) was performed to produce a barcoded, full-length cDNA from poly-adenylated mRNA. After incubation, GEMs were broken, and the pooled post-GEM-RT reaction mixtures were recovered, and cDNA was purified with silane magnetic beads (DynaBeads MyOne Silane Beads, PN37002D, ThermoFisher Scientific). The entire purified post GEM-RT product was amplified by PCR. This amplification reaction generated sufficient material to construct a

3' cDNA library. Enzymatic fragmentation and size selection was used to optimize the cDNA amplicon size and indexed sequencing libraries were constructed by End Repair, A-tailing, Adaptor Ligation, and PCR. Final libraries contain the P5 and P7 priming sites used in Illumina bridge amplification. Sequence data was generated using Illumina's NovaSeq 6000. Approximately 2000 cells were sequenced from each subject. Cell Ranger (version 2.1.1; 10x Genomics) was used for demultiplexing and alignment with default parameters. Reads were aligned to the human reference genome GRCh38 (Ensembl 93). The Seurat R package (37) was used to further process the gene counts obtained from the CellRanger pipeline. Cells that express < 200 genes, > 2500 genes, and > 5% mitochondrial genes were filtered out. Genes expressed in < 3 cells were filtered out. Gene counts were per-cell normalized and $\log_2$-transformed. These preliminary filtering and selection procedures yielded a set of 9368 sequenced cells, approximately equally distributed between subjects (and hence conditions), and 14017 genes. Note that sample collection, processing and sequencing were performed in one batch, leading to extremely high-quality data where no subject specific patterns were observed.

Classification into subpopulations using modularity-optimized Louvain community detection, and cluster labeling

Cells were classified into subpopulations using modularity optimized community detection, implemented in the Seurat R package (37). 664 highly variable genes were used to identify 10 principal components that explained the majority of variance in the data. These principal components were used to cluster the data. Clustering yielded 16 subpopulations. Cluster markers were identified using MAST (38). As suggested in (39), CIBERSORT (40) was used to "deconvolute" the average gene expression of each cluster into the constituent canonical cell types. A reference expression set of 22 immune cell types and 547 genes was used (40). Over-representation analysis was performed using the implementation of the hypergeometric test in the R package clusterprofiler with Kyoto Encyclopedia of Genes and Genomes

(KEGG) gene sets downloaded from MSigDb (41-43). Gene sets were identified as significantly over-represented if the Bonferroni-adjusted p-value was < 0.05.

scBONITA algorithm for development of discrete-state models of pathways

Network topologies: ScBONITA infers Boolean regulatory rules/ logic gates for directed networks wherein nodes represent genes and edges represent the regulatory relationships between those genes. These networks contain edge annotations denoting activation/inhibition relationships between nodes, which are exploited by scBONITA to restrict the search space for rule inference to sign-compatible canalyzing functions. Such network models of biological pathways are commonly obtained from pathway databases such as KEGG and WikiPathways (43-45). ScBONITA offers an interface to KEGG and WikiPathways databases that allows automated download and processing of user-specified networks. Users can also provide custom networks in graphml format.

Boolean rule determination from scRNA seq data: The underlying principle of scBONITA is that cross-sectional measurements of cells by scRNA-seq data represent states of an underlying dynamic biological process. scBONITA's rule determination (scBONITA-RD) algorithm, which has been extended from our previous BONITA algorithm exploits this property to infer Boolean rules for an input biological network, using a combination of a genetic algorithm (GA) and a node-wise local search (46).

The global search using GA infer a single candidate rule set that adequately describes the input data with respect to the network topology with minimum error (24, 47). The function to be minimized is:

$$\sum_{c=1}^{cells} min\left(\sum_{n=1}^{nodes} |E_{c,n} - A_{c,n,a}| \ \forall\, a \ in \ T_c \right)$$

Where, *c* from *1* to *cells* iterates over the number of cells in the training dataset, n iterates from 1 to number of *nodes* in the network, $E_{c,n}$ is the binarized expression of node *n* in cell *c*, $A_{c,n,a}$ is the value of node *n* in the attractor *a* reachable from cell *c*, and T_c is the attractor reachable from *c*. Note that T_c may have multiple repeating states in a limit cycle or only one steady state, i.e., it may be a singleton attractor. T_c is obtained after simulating the network with the candidate rule set for 100 time-steps, which causes the simulation to reach an attractor state for all tested networks.

The minimum error rule set identified using the above-described genetic algorithm strategy is further refined by a node-level local search that sequentially optimizes the rule for each node keeping the rules for all other nodes in the network constant. An optimal set of rules for a node *n* is obtained by minimizing the function

$$\sum_{c=1}^{cells} min\ (|E_{c,n}\ -\ A_{c,n,a}|\ \forall\ a\ in\ T_c)$$

where variables and constants are same as described above.

Several rules may satisfy the termination criteria with equal errors. The local search thus returns a set of equivalent rules that all satisfactorily explain the observed state in the experimental data. This set of rules is referred to as the equivalent rule set (ERS) in the text.

Pathway analysis (PA) with scBONITA: scBONITA performs pathway analysis in a two-step process. In the first step, importance scores for each node in the biological network under consideration are calculated. In the second step, a pathway modulation metric incorporating both experiment-specific fold changes and the node importance scores calculated in step 1 is calculated.

scBONITA quantifies the influence I_n of a node n over the state of the network by quantifying the overall effect of its perturbation on that network. This is achieved by simulating knock-in and knock-out of that node.

$$I_n = \sum_{c=1}^{cells} |KI_{c,n} - KO_{c,n}| * Uncertainty\ Factor$$

where $KI_{c,n}$ and $KO_{c,n}$ are the discrete expression vectors of network nodes in the attractors reached after a simulation starting from cell *c* where the node under consideration *n* is knocked in and knocked out respectively. The uncertainty factor is defined as follows:

$$\text{Uncertainty factor} = \frac{|Maximum\ ERS_i| - |Observed\ ERS_i| + 1}{|Maximum\ ERS_i|}$$

Where ERS_i is the ERS for a node *i*, $|Maximum\ ERS_i|$ is the maximum possible size of the ERS for a node *i* and $|Observed\ ERS_i|$ is the size of the ERS for a node *i* upon optimization by scBONITA.

The uncertainty factor weighs I_n relative to the maximum state space for that node, to capture the uncertainty in the rule determination for that node. The importance scores of the nodes in a network are scaled to *[0, 1]* by dividing by the maximum calculated importance score for the network under consideration.

A pathway modulation metric (M_p) is calculated by weighting the node importance score by the difference between the average gene expression in each group (relative abundance, *RA*) and the standard deviation of expression of that gene (σ). A p-value is calculated by bootstrapping, where a contrast-specific distribution of weighted importance scores is generated using randomly resampled *RA* values. Pathways are described in the text as being overall upregulated in a given contrast if the sum of fold changes of all genes in the pathway is positive. Conversely, pathways are described as being downregulated if the sum of fold changes of all genes in the pathway is negative.

$$M_p = \sum_{n=1}^{nodes} RA_n * \sigma_n * I_n$$

Pathways are described in the text as being overall upregulated in a given contrast if the sum of fold changes of all genes in the pathway is positive. Conversely, pathways are described as being downregulated if the sum of fold changes of all genes in the pathway is negative.

Steady-state analysis with scBONITA: scBONITA assumes that the observed cellular states are defined by states of multiple dynamic cellular processes or signaling pathways. While observed cells are samples along a dynamic trajectory of signaling cascades, analyzing attractors upon randomly sampling the rules from ERS allows us to investigate most common signaling states of a network under consideration. Hence, we sample ten network specific from the ERS inferred by scBONITA-RD to identify a set of reachable attractors. This is achieved by simulating the network synchronously as performed in other studies (48-51) starting from an observed state (i.e., a cell expression vector) until a steady state (or an attractor cycle) is reached. By starting simulations from expression levels of all cells (all observed states), we can ensure that these simulations cover a large fraction of available state space for a given network. In this way, all reachable attractor states, corresponding to observable signaling states, can be identified. The similarity between cells and attractors is quantified using the Hamming distance. Cells are assigned to the attractor that is most similar to their expression data.

Implementation and availability: scBONITA is implemented in Python 3 and C. Source code, documentation, and tutorials are available on https://github.com/Thakar-Lab/scBONITA.

Application of scBONITA on a publicly available data set

A scRNA-seq dataset obtained from four persons living with HIV (PLWH) before and during infection was selected to demonstrate the utility of the scBONITA pipeline on other datasets and to compare signaling dysregulations upon atherosclerosis in PLWH with signaling dysregulations upon HIV infection (36). Log2-transformed TPM data and metadata processed and curated by the study authors was collected from the Single-Cell Portal database (https://singlecell.broadinstitute.org/single_cell/study/SCP256.). The complete scBONITA pipeline was used to compare samples collected before infection to samples

collected 1 year after infection. We retained the cluster labels assigned by the authors of the original study. A set of 210 KEGG networks was used with the scBONITA pipeline. Dysregulated pathways and steady states identified by scBONITA were compared to the original analysis, as described in the results.

In silico evaluation of scBONITA

To show that scBONITA-RD is robust to training set size, we selected a cluster of B cells from the HIV/AS dataset. This subset of the dataset was manipulated to either downsample or augment the size of the training dataset (number of cells) presented to scBONITA-RD. The training dataset was downsampled to 1% and 50% of the original number of cells for cluster 0 ("B cells naïve – 1"). To augment the dataset and thereby introduce heterogeneity, the dataset was increased to 200% of its original size by adding in cells from a neighboring cluster of B cells. A set of 210 KEGG networks was used to evaluate the sizes of the ERS obtained by scBONITA-RD using these manipulated training datasets. The size of the ERS is used as a proxy for scBONITA's ability to successfully cut down the state space of the possible rules for each node using cross-sectional scRNA-seq data.

Results

Single-cell sequencing identifies 16 transcriptionally distinct cell subpopulations in PBMCs derived from AS+ and AS- PLWH

To investigate dysregulated immune signaling in People Living with HIV (PLWH), who are at an increased risk of atherosclerosis (AS), we recruited a cohort of eight PLWH, four with carotid plaques on both sides of the arteries (referred here as AS+) and four without carotid plaques (referred as AS-). Lipid profiles and age, both known risk factors for cardiovascular disease, were matched and were not significantly different between subject groups (see Methods, Supplementary File 1, Supplementary Figure 1). We used the 10X Genomics platform to profile transcriptional changes in ~1200 peripheral blood mononuclear cells (PBMCs) per subject. This scRNA-seq data was processed using the Cell Ranger and

Seurat pipelines (37) as described in the Methods to identify sixteen transcriptionally distinct populations of immune cells (Figure 1A). These clusters were then annotated using CIBERSORT (40) with a dataset of sorted immune cells (Supplementary File 1, Supplementary Figure 2) and by using cell-lineage specific markers (Supplementary Table 1). This scRNA-seq dataset is referred to in the text as the HIV/AS dataset.

A population of CD8 T cells/NK resting cells was significantly lower in AS- PLWH and a population of CD14+CD16+ monocytes was significantly higher in AS- PLWH (t-test, $p < 0.05$) (Figure 1B). The cluster-specific differentially expressed genes, or cluster markers, for these populations of CD14+CD16+ monocytes and CD8+ T cells/NK resting cells were involved in pathways linked to cell migration, such as the leukocyte transendothelial migration, regulation of actin cytoskeleton, adherens junction, and chemokine signaling pathways (Supplementary Table 1), suggesting that CD8+ T cells/NK resting cells and monocytes have a migratory phenotype. Indeed these cells are known to migrate into intima during the formation of atherosclerotic lesions in the vascular wall (52-58).

Characterization of peripheral blood mononuclear cells in people living with HIV with and without atherosclerosis

To characterize the expression differences between these cell types in AS+ and AS- PLWH, differentially expressed (DE) genes were identified using the Wilcoxon test as described in the Methods (selected cell types are shown in Figure 1C-F and complete list of DE genes presented in Supplementary Table 2). Genes were reported as being differentially expressed if the adjusted p-value was < 0.05 and the average absolute log fold-change was > 0.3 (representative cell subpopulations shown in Figure 1C-F). Gene set enrichment analysis was performed as described in the Methods. We used gene sets obtained from KEGG and curated in MSigDb. Complete results of the enrichment analysis are presented in Supplementary Table 2.

Considered together, differential expression analysis and gene set enrichment analysis provided insights into the functional differences in cells obtained from AS+ and AS- PLWH. Several genes (and gene sets) related to cell migration and mobility were upregulated in cells derived from AS+ PLWH. MHC Class 1 genes (HLA-A, HLA-B and HLA-C) and MHC Class II genes (HLA-DP, HLA-DQ, HLA-DB, and HLA-DR) were upregulated in multiple cell subpopulations. Figure 1E shows the expression of HLA-A and HLA-DRA in B cells naïve -2. Similarly, ITGB2 was upregulated in population a cluster of CD8+ T cells ("T cells CD8 – 3") derived from AS+ PLWH. These cell-surface proteins are all involved in cell-cell interactions and cellular adhesion.-ITGB2 interacts with ICAM2 expressed on the surface of endothelial cells and is involved in leukocyte transendothelial migration. The actin gene ACTB was upregulated in both populations of naïve B cells and a population of CD8+ T cells derived from AS+ PLWH. Similarly, CXCR4 was upregulated in cells derived from AS+ PLWH in two populations of naïve B cells, two populations of CD8+ T cells, and a population of resting NK cells. Both CXCR4 and ACTB play an important role in the process of leukocyte transendothelial migration. CXCR4 activation is known to drive both migration and proliferation of vascular cells. Leukocyte transendothelial migration involves dynamic actin (ACTB) cytoskeleton remodeling, that is in part mediated by the key genes RHOA and ROCK, which are not themselves differentially expressed between cells derived from AS+ and AS-PLWH. However, gene sets related to this process were not significantly over-represented in the differentially expressed genes for any subpopulations, with the exception of a small population of NK resting cells.

The S100A8/S100A9 genes are upregulated in T cells CD8/NK resting cells (Figure 1C), monocytes (Figure 1D), T cells CD8/CD4/CD4 naive (Figure 1E) and B cells naive – 2 cluster (Figure 1F) derived from AS- PLWH. S100B is upregulated in CD8+ T cells populations derived from AS- subjects (Figure 1C, 1F). In monocytes, S100B has been shown to engage RAGE leading to overproduction of reactive oxygen species, leading to the modulation of genes involved in inflammatory processes and adhesion to vasculature (59). In addition, several ribosomal genes are upregulated in cells derived from AS- PLWH in

the B cells naïve –2 cluster (RPL8, RPS10, RPS26, RPS4Y1, RPS9), and upregulated in cells derived from AS+ PLWH in the T cells CD8/CD4/CD4 naïve cluster (RP11-347P5.1, RPL13, RPL39, RPS14, RPS27, RPS29, RPS6). The ribosome gene set was over-represented in the DE genes for 12 out of the 16 identified subpopulations (Supplementary Table 2). Ribosomal genes have been associated with cellular states (60) and with the activity of the mTOR pathway (61-64).

While DE and enrichment analysis indicated some mechanisms of HIV-associated atherosclerosis, a cohesive understanding of how these multiple genes (DE and non-DE) jointly regulate signaling cascades did not emerge from the analysis above. Hence, we developed the network-based pathway analysis algorithm scBONITA to further investigate the importance of specific genes and their role in signaling.

scBONITA algorithm for development of discrete-state models of pathways

To investigate dysregulated immune signaling, we used a discrete-state modeling approach to develop executable models of signaling pathways. Specifically, we developed the scBONITA (Single-Cell Boolean Omics Network Invariant-Time Analysis) algorithm using our previously established and validated BONITA algorithm for scRNA-seq data (24) (Figure 2). Briefly, scBONITA uses a Boolean framework where “AND” or “OR” logic gates are optimized to model signal integration and flow through biological networks. scBONITA requires two inputs: (a) a binarized scRNA-seq dataset, and (b) a prior knowledge network (PKN) (Figure 2A). PKNs describe pathway topology defined by nodes representing genes and directed edges representing the activating or inhibitory interactions between nodes. The optimized logic gates for a PKN are referred to as the rule set for that PKN. scBONITA leverages the principle that observed states of single cells correspond to the steady states or attractors of dynamic biological networks to identify regulatory rules for the input PKNs (Figure 2B). A genetic algorithm is used to perform a global search and identify a minimum-error rule set which is further optimized by a node-wise local-search. This procedure returns a set of discrete-state models for pathways referred to as

the equivalent rule set (ERS). A pathway is described in the text as 'optimized' if scBONITA-RD successfully cuts down the state space of the possible rules for at least one node in the pathway.

The discrete-state models learned by scBONITA can be simulated to generate time-course trajectories that are analogous to signal flow. They can also be perturbed *in silico* by simulation of gene knock-ins and knockouts. We quantify the difference between network states after knock-out and knock-in, and weight the score by the size of the ERS to quantify the uncertainty in rule determination for each node to calculate a node-importance score that describes the influence of each node over the network. scBONITA uses these node importance scores and comparison-specific fold changes from the scRNA-seq data used for training to identify dysregulated pathways in a pre-specified contrast (Figure 2C). The simulation trajectories of these discrete-state models fall into steady states known as attractors. These attractor states of biological networks are the cell states with respect to specific pathways and have been hypothesized to correspond to signaling behavior characteristic of specific cell types. Cells are assigned to the attractor that is most similar to their expression data (Figure 2D). In this way, cells are matched to characteristic signaling states for the network under consideration. Thus, scBONITA allows in depth investigation and simulation of known biological signaling pathways by incorporating network topology.

scBONITA identifies dysregulated pathways in T cell populations in people living with HIV stratified by atherosclerosis

The scBONITA pathway analysis algorithm identifies dysregulated pathways in all subpopulations derived from AS+ and AS- PLWH, providing an insight into mechanisms of atherosclerosis development in PLWH (Supplementary Table 3). ScBONITA optimized multiple pathways in CD8+ T cells that are involved in this proinflammatory and anti-viral process (Figure 3A, Supplementary Table 3). These pathways include the JAK-STAT signaling pathway, the TGFβ signaling pathway, the NFκB signaling pathway, the AGE-RAGE signaling pathway, and the HIF-1 signaling pathway. In conjunction, cell-migration pathways such as the regulation of actin cytoskeleton and axon guidance, the PI3K-AKT

signaling pathway and mTOR signaling pathway that modulate apoptosis and cell migration, are identified as being dysregulated in the HIV+AS+ vs HIV+AS- contrast (Figure 3A). Only the Th17 cell differentiation pathway was overall upregulated in cells derived from AS+ PLWH. All these pathways were newly identified by scBONITA, i.e., the corresponding gene sets were not identified as being enriched in the AS+/AS- contrast by enrichr (Supplementary Table 2).

Pathway analysis with scBONITA identified multiple optimized pathways in subpopulations containing CD4+ T cells (T cells CD4 memory resting/T cells CD8, T cells naïve, and T cells CD4 -1 clusters, Figure 1A) as being dysregulated (Bonferroni-adjusted p-value < 0.01) in the HIV+AS+ vs HIV+AS- contrast (Figure 3B, Supplementary Table 3). CD4+ T cells may exert either an atherogenic or atheroprotective phenotype, depending on subset and interactions with antigen presenting cells (APCs), such as B cells in the adventitia or macrophages in plaques (65). Of the dysregulated pathways, herpes simplex virus 1 infection and MAPK signaling pathways were overall upregulated in T cells CD4 memory resting/ T cells CD8 and T cells CD8/CD4/CD4 naïve cells derived from AS+ PLWH. The proteoglycans in cancer and mTOR signaling pathways were overall upregulated in T cells CD4 memory resting/ T cells CD8 from AS+ PLWH. PI3K-AKT signaling and chemokine signaling pathways were upregulated in the T cells CD8/CD4/CD4 naïve cluster derived from AS+ PLWH. The ‘proteoglycans in cancer’ signaling pathway is involved in cell adhesion and migration is upstream of processes known to be dysregulated in atherosclerosis, such as regulation of the actin cytoskeleton, mTOR signaling, and apoptosis. Similarly, the herpes simplex virus infection process involves activation of the PI3K-AKT signaling and apoptosis pathways, which are known to be relevant in atherosclerosis.

The AGE-RAGE signaling pathway was further investigated in CD8+ T cells due to their relevance in atherosclerosis and to demonstrate the additional information obtained from scBONITA in comparison to other enrichment methods. The AGE-RAGE signaling pathway in a cluster of CD8+ T cells had the highest pathway modulation score (0.8) amongst all tested pathways for this cluster (Supplementary Table 3). Most of the genes in this pathway were higher in AS+ PLWH (Figure 3C). Furthermore, the

uncertainty score was used to identify pathways where logic gates for genes could be optimized. Particularly, scBONITA learned rules for the highly central DIAPH1 node, which has a high influence over signal flow in this network due to its high connectivity (uncertainty score= 0.5) (Figure 3C). The combination of scBONITA's node importance score and a difference in expression between the HIV+AS+ and HIV+AS- groups was used to identify key genes which may or may not have a significant difference in expression but whose activity influences the flow of signal through the network and the signaling behavior in atherosclerosis. These key genes in AGE-RAGE pathway had higher expression in AS+ PLWH. scBONITA assigns the class 1 PI3K genes (PIK3CA, PIK3CB and PIK3CD genes), the P13K regulator PI3KR1, and PLC genes (PLCB1, PLCB2) maximal importance scores in this network. All these genes are highly expressed in AS+ PLWH (Figure 3C). PI3K is known to activate intracellular pathways involved in the pathophysiology of atherosclerosis, such as lipid accumulation and transport, macrophage autophagy, phenotypic transition, and the expression of adhesion molecules involved in the inflammatory response (reviewed in (66)). As noted in the preceding section, P13K is also downstream of CXCR4, which is significantly upregulated in cells derived from AS+ PLWH. While CXCR4 is not itself in this network topology, scBONITA nevertheless identifies its downstream effectors PI3K and PLC, which are not themselves significantly differentially expressed, as playing an important role in the signaling pathways leading to the expression of atherosclerosis-related genes and hence and atherosclerotic phenotype. In this manner, pathway analysis with scBONITA revealed that several pathways and genes associated with atherosclerosis are dysregulated in T cells derived from PLWH. Many of these pathways have been previously shown to regulate T cell migration during atherosclerosis.

scBONITA identifies dysregulated pathways in monocytes in people living with HIV, stratified by atherosclerosis

Pathway analysis with scBONITA identified multiple optimized dysregulated pathways in monocytes (Figure 4A, Supplementary Table 3). Key pathways include the apoptosis, cAMP signaling, leukocyte

transendothelial migration, PI3K-AKT signaling and cellular senescence pathways, which appear to be involved in the proinflammatory behavior of proatherogenic monocytes.(53, 67-76). Only the cAMP signaling pathway and the endocrine resistance pathway are overall upregulated in cells derived from AS+ PLWH.

The leukocyte transendothelial migration pathway was further investigated as monocyte migration outside the vascular compartment plays a crucial role in the inflammatory cascade that leads to an atherosclerotic phenotype (67, 69, 77). In addition, scBONITA was able to learn a limited set of regulatory rules for the influential, highly connected RHOA gene (uncertainty factor=0.13). This pathway had a pathway modulation score of 0.45, which is the third-highest pathway modulation score amongst tested pathways for this cluster (Supplementary Table 3) (Figure 4B). scBONITA also assigned high importance scores to the NCF genes (NCF1, NCF2, and NCF4), CYBA and CYBB. NCF genes are involved in superoxide production and are a positive regulator of P13K signaling (78, 79). Once again, PLCG1 and PLCG2 are assigned high importance scores by scBONITA in this network, underscoring the importance of PLC in proinflammatory and proatherogenic processes. The upstream regulator of PLCG1, MSN, is involved in cytoskeletal remodeling during leukocyte migration and is similarly assigned a high importance score (80). ROCK2 shows only a small change across AS groups, which may be driven by feedback regulation of mRNAs of ROCK genes but has a high importance score indicating a stronger role in regulating the signal flow. The G protein GNAI3, which is downstream of CXCR4, is also assigned a high importance score, possibly indicating a role for CXCR4-mediated activation of this pathway despite the low observed fold change of CXCR4 between the AS+ and AS- groups. The downstream effectors of these high-importance genes have higher fold changes than the high-importance genes themselves. These genes include ACTG1 and EZR, which are involved in cytoskeletal remodeling (80-82), and ITGA4, ITGB1, and ITGB2, which are involved in cell adhesion. As in the case of CD8+ T cells, pathway analysis with scBONITA identifies several genes known to be associated with atherosclerosis which are also dysregulated in monocytes derived from PLWH.

Pathways dysregulated by HIV infection are implicated in atherosclerosis

To identify the biological mechanisms modulated by HIV infection we analyzed PBMCs from four individuals before and during acute HIV infection. Specifically, Kazer et al (36) sequenced PBMCs from 4 individuals before and during acute HIV infection and identified gene expression programs activated in proinflammatory T cells, monocytes, and NK cells during HIV infection. Pre-clustered scRNA-seq data and the set of KEGG networks used in the above analysis were used with scBONITA to infer Boolean rules and perform pathway analysis. We compared pathways that were dysregulated pathways after 1 year of HIV infection (36) to those identified as being dysregulated ($p_{adj} < 0.1$) in the AS+HIV+ vs AS-HIV+ contrast from our dataset described above (Figure 6A). Subpopulations of immune cells in the two datasets were matched for the purpose of this comparison as shown in Supplementary Table 6, except for dendritic cells, which did not have a matching subpopulation in the HIV/AS dataset.

scBONITA identified 10 optimized pathways that were dysregulated after 1 year of HIV infection in cytotoxic T cells (36) (Figure 3A-B, Figure 6A, Supplementary File 1, Supplementary Figure 5, Supplementary Table 5, Supplementary Table 6). Of these pathways, the 'Axon guidance', 'MAPK signaling', 'Proteoglycans in cancer', 'Herpes simplex virus 1 infection', and 'Cytokine-cytokine receptor interaction' signaling pathways were also dysregulated in PLWH with AS. Similarly, 5 out of 19 optimized pathways were dysregulated in monocytes upon HIV infection and in AS+ individuals (Figure 4A, Figure 6A, Supplementary File 1, Supplementary Figure 5, Supplementary Table 6). The herpes simplex virus 1 infection, PI3K-AKT signaling, and cellular senescence pathways were dysregulated upon HIV infection and in PLWH with AS. While overall dysregulation of the pathways is a crude metric for activation, we note that 81 and 41 genes from these overlapping pathways were upregulated in both contrasts in the cytotoxic T cell populations and monocyte population respectively (Figure 6B and 6C, statistical significance was not tested). Enrichment analysis using KEGG biological pathways suggests that the genes upregulated after HIV infection and in AS+ PLWH in the CD8+ T cell subpopulation were

enriched for viral response pathways such as herpes simplex virus 1 infection and human cytomegalovirus infection (Supplementary File 1, Supplementary Figure 6). Similarly, the genes upregulated after HIV infection and in AS+ PLWH in the monocyte subpopulation were enriched for cell migration related pathways such as the PI3K-AKT signaling pathway and the cAMP signaling pathway (Supplementary File 1, Supplementary Figure 6). In this vein, mTOR signaling was dysregulated in T cells from both datasets and proteoglycans in cancer, PI3K-AKT signaling, and cellular senescence were dysregulated in B cells from both datasets. These dysregulated pathways suggest that the modulation of cell migration and inflammation processes upon HIV infection progresses over time, leading to AS in PLWH.

Attractor analysis reveals PI3K genes driving distinct cellular signaling states potentially associated with atherosclerosis

We performed attractor analysis for the pathways significantly dysregulated between AS+ and AS- PLWH in the cluster of CD8+ T cells discussed above (Cluster CD8 T cells -1 in Figure 1A). The attractor analysis facilitates evaluation of cellular states across subjects and disease groups. The simplest rules, which have the smallest number of "AND" terms, were chosen to simulate the network and identify attractors as described in the Methods. The insulin resistance pathway, which is downstream of the AGE-RAGE signaling and the PI3K-AKT pathways, was particularly interesting because more than 50% of the same cluster of CD8+ T cells mapped to three dominant attractors. scBONITA identified 72 attractors representing cellular states with respect to the insulin resistance pathway in CD8+ T cells. Of these 72 signaling states, 3 dominant signaling states mapped to 16.5%, 7.5% and 27.4% of cells respectively (Figure 5A-B). The insulin resistance pathway was found to have a significant association between identified attractors and subjects (chi-square test, p-value < 0.05) but no significant association between identified attractors and atherosclerosis status (chi-square test, p-value > 0.05). Notably, attractor analysis showed that there was significant association between assigned attractors and subject from which cells were derived for the T cells CD4 - 1and T cells CD8/CD4/CD4 naïve clusters for the chemokine signaling

pathway (chi-square test, $p < 0.01$). The attractors of the PI3K-AKT signaling pathway were significantly associated with subject for the T cells CD8/CD4/CD4 naive cluster (chi-square test, $p < 0.01$).

These cellular states were characterized by differences in several key genes (Figure 5C), including PI3K genes (PI3KA, B, and D) and the PI3K regulators (PIK3R1, 2, and 3) that were identified as being highly influential in the AGE-RAGE signaling pathway (Figure 3B). In addition, the two less abundant attractors differed in the activity of the key TNFR and TNF genes. Hence, these attractors are referred to as the PIK3R+ PIK3+, TNFR+TNF- and TNFR-TNF+ attractors. The activity of these PI3K genes and the activity of AKT genes (AKT1, 2 and 3) was higher in the most common signaling state (PI3KR+ PI3K+ attractor). However, the activity of the downstream targets of AKT, such as CREB1, CREB3, CREB5, NFKB1, FOXO1, CREB3L4 and CREB3L42 were lower in the PI3KR+ PI3K+ attractor. TNF, which is known to be produced at a low level by some subsets of T cells, also mediates a range of pro-inflammatory processes in vascular endothelial cells, particularly leukocyte adhesion and transendothelial migration (83, 84). TNF-TNFR1 signaling mediates an apoptotic process that is mediated by TRADD and FADD (85). In addition, TNFR1 is known to activate the PI3K signaling pathway in regulatory T cells in the context of autoimmune disease (86). These differences may indicate differences in TNF production and response in the cells that are assigned to these cell states. Significant differences in signaling modes of cells exist across subjects, suggesting the existence of distinct modes of operation (Figure 5D).

Attractor analysis of the leukocyte transendothelial migration pathway in monocytes revealed 9 attractors that mapped to cells in the dataset and two dominant signaling modes mapping to 51.04% and 30.73 % of cells respectively (Figure 6A-B). The two dominant signaling modes of this pathway in monocytes differed in the activity of the PECAM1 and F11R genes (Figure 6C) and are hence referred to as the PECAM+ and F11R+ attractors. F11R is required for platelet adhesion to vascular endothelial cells (87), which occurs prior to infiltration of monocytes into the endothelium and eventual plaque formation (88, 89). PECAM1 has been recognized as an influential signaling molecule with widespread effects on vascular biology and atherosclerosis in particular (90-92). Attractors for this pathway were significantly

associated with the subjects (chi-square test, p-value < 0.05, Figure 6 B), but were not significantly associated with atherosclerosis status (chi-square test, p-value > 0.05). Similarly, the attractor activity of individual genes was not significantly associated with atherosclerosis status (t-test, p-value > 0.05). However, we observed significant variation in attractor activity for PECAM1 and F11R across subjects, reflective of the different states of the cells across subjects. Thus, scBONITA allows us to investigate cellular states potentially associated with inter-subject variability, driven by molecular signaling.

Evaluation of scBONITA performance in silico

The BONITA algorithm has already been rigorously validated in our previous study (24). Specifically, comparison with other network-based pathway analysis tools has been performed. Here we evaluate scRNA-seq specific components of the algorithm. To show that scBONITA rule determination is robust to training set size, we varied the size of the training data provided to scBONITA. Specifically, the number of cells in the largest cluster of cells (Naïve B cells -1) were varied by random selection from 1% of cells from that cluster to 200% by adding cells from neighboring clusters. The reduced size of the ERS for nodes with in-degree 3 (i.e., the most complex case considered by scBONITA) informs improved certainty in rule inference by scBONITA. (Figure 7A) While there was a significant decline in performance when the data was downsampled to 1% of the original cluster, there was no significant increase in effect once 50% of the cells were used, or when the training dataset was augmented. This indicates that scBONITA is robust to heterogeneity in the training data set. To show that scBONITA's node importance score is not correlated to commonly used measures of node centrality, we compared the node importance scores calculated by scBONITA for KEGG networks when it is trained on the HIV/AS dataset as described above to six centrality measures – Katz centrality, degree centrality, current flow centrality, eccentricity centrality, betweenness centrality, and local reaching centrality. We observed that scBONITA's node importance score is not correlated to any of these metrics (Spearman Correlation Coefficient < 0.15, Figure 6H). To show that network topology also significantly influences the node importance score, we compared scBONITA's node importance scores for the same set of KEGG

pathways, assigned using different training datasets. These node importance scores were compared using similar cell subpopulations only. We found that the node importance scores between the two datasets were correlated as shown by a representative comparison between the node importance scores for the subpopulation of cytotoxic T cells from the Kazer et al dataset and the subpopulations of CD8+ T cells (Figure 6B, $0.71 < \text{Pearson Correlation Coefficient} < 0.91$, $p < 0.01$) show .Similarly, the node importance scores for the populations of monocytes were highly correlated (Pearson correlation coefficient = 0.78, Supplementary Table 4, Supplementary File 1, Supplementary Figure 3). However, the correlations were relatively lower for other pairs of subpopulations (Supplementary Table 4, Supplementary File 1, Supplementary Figure 5), indicating that scBONITA learns some characteristic features of a network topology, but node importance scores are still assigned in a context-dependent manner.

Discussion

Among people living with HIV, widespread use of cART has significantly reduced overall mortality. However, the earlier and increased incidence of cardiovascular diseases, including atherosclerosis, remains the major cause of mortality in an aging HIV+ population. The causes for this are manifold and include side effects of cART and lower level of HIV proliferation (4, 9-12). We and others have attempted to identify the immune signaling mechanisms that lead to this increased incidence of atherosclerosis (93). However, to the best of our knowledge no study has attempted to holistically study the combined effects of variance in the numbers of specific immune cells and the cell-type specific signaling dysregulations (93). We found that in accordance with previous studies (19, 94-100), a population of CD8+ T cells was significantly increased in PBMCs from AS+ PLWH. However, contrary to our expectations (20, 68, 69, 74, 76, 101-104), a population of monocytes was significantly *decreased* in PBMCs from AS+ PLWH. Interestingly, evaluation by our pathway analysis algorithm scBONITA and differential expression analysis identified differences in the migratory phenotype of these cells, suggesting to us that these monocytes are migrating into the vascular intima in AS+ PLWH (described

later in the discussion). Conventional differential expression and gene set enrichment analysis methods identified genes involved in signaling pathways that are known to be linked to cell migration and cell aging. Key amongst these identified genes were CXCR4 and ACTB (Figure 1 C-F) which were upregulated in populations of CD8+ T cells derived from AS+ PLWH. CXCR4 activation by its ligands leads to the activation of phosphatidylinositol-3-OH kinases (PI3K), which in turn leads to the activation of the serine-threonine kinase AKT via PIP3 (105). PI3K/AKT signaling leads to multiple processes involved in plaque formation, such as cell migration, intracellular lipid accumulation, and smooth muscle cell proliferation (66). S100A8/S100A9 were found to be upregulated in monocytes derived from AS-PLWH (Figure 1 C-F). In monocytes, S100A8/9 have been shown to increase adhesion, migration, and production of inflammatory cytokines such as TNF-alpha and IL1β (106, 107). However, none of these processes were identified as being significantly enriched in the differentially expressed genes from these subpopulations. In addition, these methods failed to provide insights into how disparate genes involved in different pathways regulate cellular states. To characterize signaling dysregulations in HIV-associated atherosclerosis more effectively, we developed the scBONITA algorithms for regulatory rule inference, network simulation, pathway analysis, and attractor/steady-state analysis.

scBONITA learns condition-specific logic models using scRNA-seq data in conjunction with published prior knowledge networks. This study builds on our previously published BONITA method (24) that inferred logic rules from bulk RNAseq data. scBONITA exploits the bimodal nature of scRNA-seq data (38, 108) and the cell-level resolution of expression to successfully learn regulatory rules and identify attractors for prior knowledge networks. We show that scBONITA can successfully learn regulatory rules for biologically significant signaling pathways and that these rules can be used to perturb and simulate these pathways *in silico*. Unlike other tools utilizing Boolean networks, scBONITA is not dependent on time-series data and in fact hypothesizes that scRNA-seq data represents samples in the state space of a dynamic Boolean network. In addition, scBONITA uses published network topologies, thereby reducing the uncertainty in the inferred rules. Other groups have published algorithms to infer logic rules and

595 reconstruct gene-regulatory networks on a small subset of genes from scRNA-seq data (51, 109, 110).
596 However, scBONITA does not depend on pre-selection of genes. Additionally, scBONITA also identifies
597 dysregulated signaling pathways in a given context, combining expression information with scBONITA
598 derived impact score to create a unique metric of pathway dysregulation that considers (a) the dynamic
599 nature of signaling pathways and (b) the impact of node perturbations.

600 scBONITA identifies interesting, dysregulated pathways across all cell subpopulations in the HIV/AS
601 dataset (Supplementary Table 3, Figures 3-4). The AGE-RAGE signaling pathway was significantly
602 dysregulated in a population of CD8+ T cells (Figure 3A). AGE-RAGE signaling elicits activation of
603 multiple intracellular signaling pathways such as cell proliferation and apoptosis pathways (111-119).
604 scBONITA assigned the highest importance scores for this network to the PI3K family of genes
605 (PIK3CA, PIK3CB and PIK3CD), which promote intracellular lipid deposition leading to the formation
606 of foam cells and atherosclerotic plaques and can also reduce the expression of lipid transporters and
607 reduce the efflux of intracellular cholesterol depending on upstream signals (66). PLC (PLCB1 and
608 PLCB2 genes), which is also assigned a high importance score in this network, facilitates
609 proinflammatory and proatherogenic processes. PLC activity induced by oxidized low-density lipids
610 (oxLDL) serves to stimulate proinflammatory IL-8 secretion and promote leukocyte adhesion, promoting
611 plaque development. PLC also enhances endothelial dysfunction and plaque progression by inducing
612 VEC apoptosis (80, 120). Of note, both PI3K and PLC genes were upregulated in AS+ PLWH (Figure
613 3C).

614 ScBONITA identified several pathways linked to lipid metabolism as being dysregulated in the
615 population of monocytes. Amongst these pathways were the cAMP signaling pathway, which was overall
616 upregulated in AS+ PLWH, and leukocyte transendothelial migration pathway, which was overall
617 upregulated in AS- PLWH, both of which are involved in the infiltration of monocytes into the intima
618 during the formation of atherosclerotic lesions and hence progression of atherosclerosis (52-57).
619 Similarly, scBONITA identified genes critical to the atherosclerotic process in the leukocyte

transendothelial migration pathway trained on the monocyte subpopulation. Specifically, ROCK1 and ROCK2 are stimulated by atherogenic stimuli, such as oxLDL. ROCK activation leads to various pathophysiological changes include endothelial dysfunction, migration and angiogenesis, migration, proliferation and differentiation in SMCs and vascular remodeling (121, 122). ROCK inhibitors such as statins have been recently shown to attenuate atherosclerosis by inhibiting ROCK1 and ROCK2 and consequently inhibition of altered chemotaxis of macrophages and its transformation into foam cells (123). The dysregulation of the glucagon signaling pathway, cAMP signaling, PI3K-AKT signaling and proteoglycans in cancer pathways indicate that in AS+ PLWH, dysregulations in glucose metabolism induce expression of adhesion molecules by the vascular endothelium resulting in increased monocyte transendothelial migration (66, 124). In this manner, scBONITA revealed novel insights into pathway regulation upon atherosclerosis.

Pathway analysis with scBONITA shows that lipid metabolism and cell migration are dysregulated in AS+ PLWH across all cell subpopulations. This effect is most clearly seen in the case of the PI3K-AKT signaling pathway, which is dysregulated in all cell subpopulations (Figures 4 – 5, Supplementary Table 3). The pathways that are upstream and downstream of PI3K-AKT signaling are, however, dysregulated in different subpopulations, suggesting that the activation and effector mechanisms of this signaling cascade vary by cell type. While there appears to be no strong evidence for apelin expression in B cells, the apelin signaling pathway was upregulated in B cells naïve -1 derived from AS+ PLWH and adipocytokine signaling pathway was downregulated in B cells naïve -2 derived from AS+ PLWH, along with PI3K-AKT signaling and MAPK signaling. The cardioprotective effect of apelin is modulated by (amongst other routes) the PI3K-AKT signaling and MAPK signaling pathways (80-82). It is also shown to be upregulated in human atherosclerotic coronary arteries and colocalized with markers for macrophages (125, 126). PI3K-AKT signaling is also dysregulated in CD4+ T cells (Figure 4B), as is its upstream signaling pathway cytokine-cytokine receptor interaction, suggesting a different mechanism of activation of PI3K-AKT signaling in this cell type.

We used the scBONITA pipeline to infer pathways involved in the progression of HIV infection from an independent, publicly available scRNA-seq dataset derived from 4 subjects before and after HIV infection and compared these pathways to those identified in the progression of atherosclerosis in PLWH. scBONITA-RD was able to successfully learn regulatory rules for KEGG pathways when trained on this dataset (Supplementary File 1, Supplementary Figure 4). Several pathways dysregulated upon HIV infection were also dysregulated in PLWH with AS (Figure 3A, Figure 4A, Supplementary File 1, Supplementary Figure 5, Supplementary Table 6). Among the dysregulated pathways, the proteoglycans in cancer pathway, which is linked to cell migration and adhesion, and the axon guidance pathway, which is linked to cytoskeletal reorganization and Rho GTPase signaling and has been suggested to be a special case of cell migration that is active in many cell types, are both also suggestive of changes occurring in cell migration of cytotoxic T cells due to HIV infection (127-130). Interestingly, both these pathways are also linked to the cytokine - cytokine receptor interaction pathway. cAMP signaling negatively regulates the production of PI3K-AKT signaling and hence the transcription of pro-inflammatory cytokines via PKA, and positively regulates the transcription of anti-inflammatory cytokines via PKA and CREB. Decreased PI3K-AKT signaling results in decreased cell migration (131). The PI3K-AKT signaling, cAMP signaling, and cellular senescence pathways were dysregulated in the population of monocytes derived after one year of HIV infection and in monocytes derived from PLWH with AS, further indicating an HIV-induced dysregulation in cell migration processes. These conclusions were further borne out by the enrichment analysis of genes from these pathways that were upregulated after HIV infection and in atherosclerosis (Figure 7).

To map cells to distinct signaling modes of the pathways described above, we developed scBONITA's attractor analysis capabilities. Attractors are regions in the state space of a dynamic system towards which simulation trajectories are "pulled" or attracted. These attractors and the propensity of simulation trajectories to end in these attractors (i.e., the size of the attractor basins) are characteristics of a specific network with a specific set of regulatory rules. Previous works have suggested that these steady states

correspond to observable cell states, or hallmarks of specific phenotypes such as cell type differentiation, disease state, or drug treatment (132-137). These studies show that even simple dynamic models capture rich and nuanced cell behaviors. ScRNA-seq allows the study of these dynamic landscapes and their steady states or attractors at an unprecedented resolution (137-139). scBONITA uses learned rules to map cells to characteristic signaling states based on the property of Boolean networks to move towards steady states or attractors. This attractor analysis allows users to characterize cells based on the dynamic properties of signaling networks, which dictate their phenotype. scBONITA not only identifies these attractors, but it also allows identification, of the master regulators or switches that control the changes between these cell states by evaluating scBONITA's node importance score. Thus, this attractor analysis provides complex insights into cellular processes in a variety of conditions.

The importance of cell migration and dysregulated lipid signaling in the development of HIV-associated atherosclerosis was further underscored by attractor analysis with scBONITA. We identified attractors for all signaling pathways that were identified as being dysregulated upon AS in PLWH in CD8+ T cells and monocytes, and mapped cells to these identified signaling states. Furthermore, we identified signaling pathways in which (a) more than one attractor mapped to a significant proportion of cells from the cluster under consideration and (b) there was a significant association between the attractor to which cells were assigned and the subject from which these cells were derived. We note that in most cases, multiple theoretically possibly signaling modes (attractors) were identified but only one dominant signaling state existed in the dataset. Using the criteria defined above, we selected the insulin resistance pathway in CD8+ T cells and the leukocyte transendothelial migration pathway in monocytes for further analysis (140-144). We also note that the insulin signaling pathway exerts immunomodulatory effects on T cells. Decreased insulin receptor expression (used as a proxy for insulin resistance) during viral infection has been shown to downregulate components of the infection response, such as proliferation, cytokine response and glycolysis (140). The three dominant signaling modes of the insulin resistance pathway differed in the activity of PI3K and AKT genes, which were identified as key regulators of the pathways

695 described in the preceding sections, and their downstream effectors, such as CREB and FOXO1. This
696 suggests the existence of two distinct modes of operation for this signaling pathway corresponding to a
697 proliferative cell state (activation of PI3K and AKT) and a senescent cell state (transcription of CREB-
698 and FOXO1-controlled genes) (141, 142, 145). Similarly, we identified two dominant signaling modes for
699 the leukocyte transendothelial migration pathway in monocytes. These modes differed in the activity of
700 F11R and PECAM1 genes, which were active in the most common and second most common attractor
701 respectively. While there is no significant separation between cells derived from AS+ and AS- PLWH
702 based on the attractors that they map to, the existence of these two signaling modes suggests variation in
703 the cell states with respect to this pathway in PLWH. Dysregulation in insulin signaling promotes
704 PECAM1-mediated migration of monocytes through endothelial cells (146, 147). Emerging evidence
705 suggests that PECAM1's loss contributes to atherosclerosis (92). The presence of a signaling state in
706 which PECAM1 is deficient may therefore indicate that those cells are contributing to a negative
707 feedback loop of the inflammatory process. The identification of pathway-specific signaling modes that
708 can be differentiated based on specific gene activities shows that scBONITA can shed light on signaling
709 mechanisms that are not apparent by analysis of gene expression differences alone.

710 Although BONITA algorithm has been rigorously validated in our prior publication (46) here we wanted
711 to evaluate the scRNA-seq data specific parts of the algorithm. We next assessed whether the provided
712 network topology also significantly influences the node importance score, and the dependence of the node
713 importance score on the training data. We demonstrated the influence of network topology on the node
714 importance score (Figure 7B), which is also an indirect measure of the similarity (though not identity) of
715 the rules inferred by scBONITA for a given network, using different datasets. Thus, scBONITA can
716 identify characteristic structural properties of networks and use this in conjunction with expression
717 information to identify dysregulated pathways in a specified condition. We also show that scBONITA's
718 node importance score is not correlated with measures of node centrality (Figure 6H). We also assessed
719 the dependence of scBONITA on the training data to show that scBONITA-RD can narrow down the vast

720 possible state space for a Boolean network (Figure 6A). This ability is dependent on the similarity of the
721 signaling process operating in the cells of the training dataset. scBONITA's ability to resolve rules
722 decreases slightly when the heterogeneity of the training dataset increases (Figure 7E, 200% cells). This
723 restricts the ability of scBONITA to identify regulatory rules that can be experimentally verified. We
724 expect that this capability will improve significantly when pure cell populations are sequenced, for
725 example after flow cytometry or pure cell culture. While scBONITA is not strictly dependent on the
726 clustering method used to classify scRNA-seq data into subpopulations, we used pre-classified
727 subpopulations to reduce variability and, additionally, to improve the specificity of scBONITA-PA by
728 restricting the identification of dysregulated pathways to cell types. This is consistent with the typical
729 gene set enrichment analysis in the context of scRNA-seq data. Additionally, scBONITA-RD requires a
730 longer runtime (<12 hours in our tests) and more powerful computational capabilities than a typical
731 analysis pipeline run on scRNA-seq dataset of typical size; however, these resources are usually available
732 to academic users on computing clusters.

733 The biological variability and nonspecific distortions of expression due to the technicalities of scRNA-seq
734 has been previously identified (148), leading to identification of fewer differences across conditions, as in
735 studies such as (149). In addition, even differential expression methods that are sensitive to the known
736 characteristic distributions of scRNA-seq data are prone to false discoveries (recently reviewed in
737 34584091). Our approach implemented in scBONITA allows analysis of genes in the context of their
738 function in the signaling pathways and network topology of the interactions. This additional information
739 minimizes the impact of the caveats in the scRNA-seq technology mentioned above. Thus, our analysis
740 reveals influential genes in several signaling networks in a context-specific manner, thereby predicting
741 novel targets for further experimental validation or for therapies.

Conclusions

To study the cellular and immunological processes involved in HIV-associated atherosclerosis, we used scRNA-seq to profile PBMCs from 8 PLWH, 4 of whom had atherosclerosis. We developed the scBONITA algorithm to use this scRNA-seq data to (a) infer regulatory rules for networks with a known topology, (b) perturb and simulate these networks *in silico* to identify master regulators of these networks, (c) combined this topology-specific information with expression information to identify dysregulated pathways in this condition, and (d) grouped cells into characteristic signaling states based on the dynamic properties of these networks. We validated scBONITA on a publicly available dataset of PBMCs from persons before and after HIV infection. scBONITA identified key dysregulated pathways that drive inflammation in people living with HIV. The scBONITA source code, along with documentation and tutorials, is freely available on https://github.com/Thakar-Lab/scBONITA.

List of abbreviations

AS: atherosclerosis; HIV: human immunodeficiency virus; PLWH: people living with HIV; PBMC: peripheral blood mononuclear cell; scBONITA: single-cell Boolean Omics Network Invariant Time Analysis; single-cell RNA sequencing: scRNA-seq; CVD: cardiovascular disease; ORA: overrepresentation analysis; cART: combined antiretroviral therapy; KEGG: Kyoto Encyclopedia of Genes and Genomes; scBONITA-RD: single-cell Boolean Omics Network Invariant Time Analysis rule determination; scBONITA-PA: single-cell Boolean Omics Network Invariant Time Analysis pathway analysis; GA: genetic algorithm; LS: local search; RA: relative abundance; ERS: equivalent rule set; PKN: prior knowledge network

Acknowledgements

We would like to thank Adam Cornwell, Jiayue Meng and George Kassis for testing scBONITA at various stages of development and for useful discussions on scBONITA functionality. We would also like

to thank Alan Grossfield, Andrew McDavid, Gourab Ghoshal, David Mathews, Lauren Benoodt, Raven M. Osborn, and all past and present members of the Thakar Lab for helpful discussions. The Center for Integrated Research Computing at the University of Rochester provided high-performance computing resources and computing expertise. We are especially grateful to the participants in the HIV/AS study, their families, and the clinical team.

Funding

The study was supported by U.S. National Institutes of Health. MGP is supported by R01 AI134058. RP is supported by T32 GM07356. JT was supported by UM1 AI069511, P30 AI078498, R01 AI134058 and R21 AI136668. SBM, GS and AT were supported by R01 HL123346, SBM and MVS are supported by R01 HL128155, R01 NS066801. The University of Rochester Center for AIDS Research (UR-CFAR; P30 AI078498) provided support and core facilities.

Declarations

Authors' information

Affiliations

[1] Biophysics, Structural, and Computational Biology Program, University of Rochester School of Medicine and Dentistry, Rochester, USA. [2] Medical Scientist Training Program, University of Rochester School of Medicine and Dentistry, Rochester, USA. [3] University of Rochester Clinical & Translational Science Institute. [4]Department of Microbiology, Immunology and Tropical Medicine, George Washington University School of Medicine and Health Sciences, Washington, D.C., USA. [5]Department of Neurology, University of Rochester School of Medicine and Dentistry, Rochester, USA. [6]Department of Imaging Sciences, University of Rochester School of Medicine and Dentistry, Rochester, USA. [7]Department of Biostatistics and Computational Biology, University of Rochester School of Medicine and

Dentistry, Rochester, USA. [8]Department of Microbiology and Immunology, University of Rochester School of Medicine and Dentistry, Rochester, USA. [9]Department of Biomedical Genetics, University of Rochester School of Medicine and Dentistry, Rochester, USA

Authors' contributions

Conceptualization of the study: JT, conceptualization of BONITA: MGP, RP, JT; Data curation: MGP, AT, JT; Formal Analysis: MGP, JT; Funding acquisition: SM, GS, JT; Investigation: MGP, JT; Methodology: MGP, JT; Project administration: AT, JT; Resources: SM, GS, MVS, JT; Software: MGP, JT; Supervision: JT; Validation: MGP, JT; Visualization: MGP, JT; Writing – original draft: MGP, JT; Writing – review & editing: All authors

Ethics Declarations

Ethics approval and consent to participate

All methods were carried out in accordance with University of Rochester guidelines and regulations, and all experimental and study protocols were approved by the University of Rochester Institutional Review Board (#RSRB00063845). All study participants gave their written informed consent.

Consent for publication

Not applicable

Availability of data and materials

The HIV/AS scRNA-seq dataset presented in this manuscript has been deposited in Single Cell Portal and will be made public upon publication of the manuscript. Due to the sensitive nature of HIV data, we have not made the raw data public; however, all results presented in this manuscript may be recapitulated from the data in Single Cell Portal. We also analyzed a previously published dataset that is freely accessible at

https://singlecell.broadinstitute.org/single_cell/study/SCP256. All source code and documentation for the scBONITA package is available at https://github.com/Thakar-Lab/scBONITA.

Competing interests

The authors declare that they have no competing interests.

References

1. McLaughlin MM, Ma Y, Scherzer R, Rahalkar S, Martin JN, Mills C, et al. Association of Viral Persistence and Atherosclerosis in Adults With Treated HIV Infection. JAMA Netw Open. 2020;3(10):e2018099.
2. Shah ASV, Stelzle D, Lee KK, Beck EJ, Alam S, Clifford S, et al. Global Burden of Atherosclerotic Cardiovascular Disease in People Living With HIV. Circulation. 2018;138(11):1100-12.
3. Althoff KN, McGinnis KA, Wyatt CM, Freiberg MS, Gilbert C, Oursler KK, et al. Comparison of risk and age at diagnosis of myocardial infarction, end-stage renal disease, and non-AIDS-defining cancer in HIV-infected versus uninfected adults. Clin Infect Dis. 2015;60(4):627-38.
4. Drozd DR, Kitahata MM, Althoff KN, Zhang J, Gange SJ, Napravnik S, et al. Increased Risk of Myocardial Infarction in HIV-Infected Individuals in North America Compared With the General Population. J Acquir Immune Defic Syndr. 2017;75(5):568-76.
5. Mdodo R, Frazier EL, Dube SR, Mattson CL, Sutton MY, Brooks JT, et al. Cigarette smoking prevalence among adults with HIV compared with the general adult population in the United States: cross-sectional surveys. Ann Intern Med. 2015;162(5):335-44.
6. Tien PC, Schneider MF, Cox C, Karim R, Cohen M, Sharma A, et al. Association of HIV infection with incident diabetes mellitus: impact of using hemoglobin A1C as a criterion for diabetes. J Acquir Immune Defic Syndr. 2012;61(3):334-40.
7. Schouten J, Wit FW, Stolte IG, Kootstra NA, van der Valk M, Geerlings SE, et al. Cross-sectional comparison of the prevalence of age-associated comorbidities and their risk factors between HIV-infected and uninfected individuals: the AGEhIV cohort study. Clin Infect Dis. 2014;59(12):1787-97.
8. Cotter AG, Satchell CS, O'Halloran J A, Feeney ER, Sabin CA, Mallon PW. High-density lipoprotein levels and 10-year cardiovascular risk in HIV-1-infected patients. Aids. 2011;25(6):867-9.
9. Fahme SA, Bloomfield GS, Peck R. Hypertension in HIV-Infected Adults: Novel Pathophysiologic Mechanisms. Hypertension. 2018;72(1):44-55.
10. Hatleberg CI, Ryom L, d'Arminio Monforte A, Fontas E, Reiss P, Kirk O, et al. Association between exposure to antiretroviral drugs and the incidence of hypertension in HIV-positive persons: the Data Collection on Adverse Events of Anti-HIV Drugs (D:A:D) study. HIV Med. 2018;19(9):605-18.
11. Triant VA, Lee H, Hadigan C, Grinspoon SK. Increased acute myocardial infarction rates and cardiovascular risk factors among patients with human immunodeficiency virus disease. J Clin Endocrinol Metab. 2007;92(7):2506-12.
12. Freiberg MS, Chang CC, Kuller LH, Skanderson M, Lowy E, Kraemer KL, et al. HIV infection and the risk of acute myocardial infarction. JAMA Intern Med. 2013;173(8):614-22.
13. Vos AG, Idris NS, Barth RE, Klipstein-Grobusch K, Grobbee DE. Pro-Inflammatory Markers in Relation to Cardiovascular Disease in HIV Infection. A Systematic Review. PLoS One. 2016;11(1):e0147484.

14. Subramanian S, Tawakol A, Burdo TH, Abbara S, Wei J, Vijayakumar J, et al. Arterial inflammation in patients with HIV. Jama. 2012;308(4):379-86.
15. Burdo TH, Lentz MR, Autissier P, Krishnan A, Halpern E, Letendre S, et al. Soluble CD163 made by monocyte/macrophages is a novel marker of HIV activity in early and chronic infection prior to and after anti-retroviral therapy. The Journal of infectious diseases. 2011;204(1):154-63.
16. Dirajlal-Fargo S, Sattar A, Kulkarni M, Funderburg N, McComsey GA. Soluble TWEAK may predict carotid atherosclerosis in treated HIV infection. HIV Clin Trials. 2017;18(4):156-63.
17. Corbeau P, Reynes J. Immune reconstitution under antiretroviral therapy: the new challenge in HIV-1 infection. Blood. 2011;117(21):5582-90.
18. Longenecker CT, Sullivan C, Baker JV. Immune activation and cardiovascular disease in chronic HIV infection. Curr Opin HIV AIDS. 2016;11(2):216-25.
19. Schäfer S, Zernecke A. CD8(+) T Cells in Atherosclerosis. Cells. 2020;10(1):37.
20. Jaworowski A, Hearps AC, Angelovich TA, Hoy JF. How Monocytes Contribute to Increased Risk of Atherosclerosis in Virologically-Suppressed HIV-Positive Individuals Receiving Combination Antiretroviral Therapy. Front Immunol. 2019;10:1378.
21. Khatri P, Sirota M, Butte AJ. Ten years of pathway analysis: current approaches and outstanding challenges. PLoS computational biology. 2012;8(2):e1002375-e.
22. Thakar J, Pilione M, Kirimanjeswara G, Harvill ET, Albert R. Modeling systems-level regulation of host immune responses. PLoS Comput Biol. 2007;3(6):e109.
23. Van Twisk D, Murphy SP, Thakar J. Optimized logic rules reveal interferon-gamma-induced modes regulated by histone deacetylases and protein tyrosine phosphatases. Immunology. 2017;151(1):71-80.
24. Palli R, Palshikar MG, Thakar J. Executable pathway analysis using ensemble discrete-state modeling for large-scale data. PLoS Comput Biol. 2019;15(9):e1007317.
25. Saigusa R, Winkels H, Ley K. T cell subsets and functions in atherosclerosis. Nature reviews Cardiology. 2020;17(7):387-401.
26. Tay C, Kanellakis P, Hosseini H, Cao A, Toh B-H, Bobik A, et al. B Cell and CD4 T Cell Interactions Promote Development of Atherosclerosis. Frontiers in Immunology. 2020;10.
27. Tse K, Tse H, Sidney J, Sette A, Ley K. T cells in atherosclerosis. Int Immunol. 2013;25(11):615-22.
28. Abdolmaleki F, Gheibi Hayat SM, Bianconi V, Johnston TP, Sahebkar A. Atherosclerosis and immunity: A perspective. Trends Cardiovasc Med. 2019;29(6):363-71.
29. Perry H, Bender T, McNamara C. B cell subsets in atherosclerosis. Frontiers in Immunology. 2012;3.
30. Srikakulapu P, McNamara CA. B cells and atherosclerosis. American Journal of Physiology-Heart and Circulatory Physiology. 2017;312(5):H1060-H7.
31. Tay C, Liu Y-H, Hosseini H, Kanellakis P, Cao A, Peter K, et al. B-cell-specific depletion of tumour necrosis factor alpha inhibits atherosclerosis development and plaque vulnerability to rupture by reducing cell death and inflammation. Cardiovascular Research. 2016;111(4):385-97.
32. Tay C, Liu Y-H, Kanellakis P, Kallies A, Li Y, Cao A, et al. Follicular B Cells Promote Atherosclerosis via T Cell–Mediated Differentiation Into Plasma Cells and Secreting Pathogenic Immunoglobulin G. Arteriosclerosis, Thrombosis, and Vascular Biology. 2018;38(5):e71-e84.
33. Tsiantoulas D, Diehl CJ, Witztum JL, Binder CJ. B cells and humoral immunity in atherosclerosis. Circ Res. 2014;114(11):1743-56.
34. Weber C, Zernecke A, Libby P. The multifaceted contributions of leukocyte subsets to atherosclerosis: lessons from mouse models. Nat Rev Immunol. 2008;8(10):802-15.
35. Zernecke A, Winkels H, Cochain C, Williams JW, Wolf D, Soehnlein O, et al. Meta-Analysis of Leukocyte Diversity in Atherosclerotic Mouse Aortas. Circ Res. 2020;127(3):402-26.
36. Kazer SW, Aicher TP, Muema DM, Carroll SL, Ordovas-Montanes J, Miao VN, et al. Integrated single-cell analysis of multicellular immune dynamics during hyperacute HIV-1 infection. Nature Medicine. 2020;26(4):511-8.

37. Butler A, Hoffman P, Smibert P, Papalexi E, Satija R. Integrating single-cell transcriptomic data across different conditions, technologies, and species. Nat Biotechnol. 2018;36(5):411-20.
38. Finak G, McDavid A, Yajima M, Deng J, Gersuk V, Shalek AK, et al. MAST: a flexible statistical framework for assessing transcriptional changes and characterizing heterogeneity in single-cell RNA sequencing data. Genome Biol. 2015;16:278.
39. Diaz-Mejia JJ, Meng EC, Pico AR, MacParland SA, Ketela T, Pugh TJ, et al. Evaluation of methods to assign cell type labels to cell clusters from single-cell RNA-sequencing data. F1000Res. 2019;8.
40. Newman AM, Liu CL, Green MR, Gentles AJ, Feng W, Xu Y, et al. Robust enumeration of cell subsets from tissue expression profiles. Nat Methods. 2015;12(5):453-7.
41. Wu T, Hu E, Xu S, Chen M, Guo P, Dai Z, et al. clusterProfiler 4.0: A universal enrichment tool for interpreting omics data. Innovation (N Y). 2021;2(3):100141.
42. Liberzon A, Birger C, Thorvaldsdottir H, Ghandi M, Mesirov JP, Tamayo P. The Molecular Signatures Database (MSigDB) hallmark gene set collection. Cell Syst. 2015;1(6):417-25.
43. Kanehisa M, Furumichi M, Sato Y, Ishiguro-Watanabe M, Tanabe M. KEGG: integrating viruses and cellular organisms. Nucleic acids research. 2021;49(D1):D545-d51.
44. Martens M, Ammar A, Riutta A, Waagmeester A, Slenter DN, Hanspers K, et al. WikiPathways: connecting communities. Nucleic acids research. 2021;49(D1):D613-d21.
45. Palshikar MG, Hilchey SP, Zand MS, Thakar J. WikiNetworks: translating manually created biological pathways for topological analysis. Bioinformatics. 2021.
46. Palli R, Palshikar MG, Thakar J. Executable pathway analysis using ensemble discrete-state modeling for large-scale data. Plos Computational Biology. 2019;15(9).
47. Fortin F-A, De Rainville F-M, Gardner M-AG, Parizeau M, Gagné C. DEAP: Evolutionary algorithms made easy. The Journal of Machine Learning Research. 2012;13(1):2171-5.
48. Méndez A, Mendoza L. A Network Model to Describe the Terminal Differentiation of B Cells. PLoS Comput Biol. 2016;12(1):e1004696.
49. Martínez-Méndez D, Villarreal C, Mendoza L, Huerta L. An Integrative Network Modeling Approach to T CD4 Cell Activation. Front Physiol. 2020;11:380.
50. Palma A, Jarrah AS, Tieri P, Cesareni G, Castiglione F. Gene Regulatory Network Modeling of Macrophage Differentiation Corroborates the Continuum Hypothesis of Polarization States. Front Physiol. 2018;9:1659.
51. Schwab JD, Ikonomi N, Werle SD, Weidner FM, Geiger H, Kestler HA. Reconstructing Boolean network ensembles from single-cell data for unraveling dynamics in the aging of human hematopoietic stem cells. Comput Struct Biotechnol J. 2021;19:5321-32.
52. Bäck M, Yurdagul A, Jr., Tabas I, Öörni K, Kovanen PT. Inflammation and its resolution in atherosclerosis: mediators and therapeutic opportunities. Nature reviews Cardiology. 2019;16(7):389-406.
53. Negreiros-Lima GL, Lima KM, Moreira IZ, Jardim BLO, Vago JP, Galvão I, et al. Cyclic AMP Regulates Key Features of Macrophages via PKA: Recruitment, Reprogramming and Efferocytosis. Cells. 2020;9(1).
54. Wahlang B, McClain C, Barve S, Gobejishvili L. Role of cAMP and phosphodiesterase signaling in liver health and disease. Cell Signal. 2018;49:105-15.
55. Sugimoto MA, Vago JP, Perretti M, Teixeira MM. Mediators of the Resolution of the Inflammatory Response. Trends Immunol. 2019;40(3):212-27.
56. Dalli J, Serhan CN. Pro-Resolving Mediators in Regulating and Conferring Macrophage Function. Front Immunol. 2017;8:1400.
57. Lorenowicz MJ, Fernandez-Borja M, Hordijk PL. cAMP signaling in leukocyte transendothelial migration. Arterioscler Thromb Vasc Biol. 2007;27(5):1014-22.
58. Gewaltig J, Kummer M, Koella C, Cathomas G, Biedermann BC. Requirements for CD8 T-cell migration into the human arterial wall. Human Pathology. 2008;39(12):1756-62.

59. Hayakawa E, Yoshimoto T, Sekizawa N, Sugiyama T, Hirata Y. Overexpression of receptor for advanced glycation end products induces monocyte chemoattractant protein-1 expression in rat vascular smooth muscle cell line. J Atheroscler Thromb. 2012;19(1):13-22.
60. Athanasiadis EI, Botthof JG, Andres H, Ferreira L, Lio P, Cvejic A. Single-cell RNA-sequencing uncovers transcriptional states and fate decisions in haematopoiesis. Nature Communications. 2017;8(1):2045.
61. Iadevaia V, Huo Y, Zhang Z, Foster Leonard J, Proud Christopher G. Roles of the mammalian target of rapamycin, mTOR, in controlling ribosome biogenesis and protein synthesis. Biochemical Society Transactions. 2012;40(1):168-72.
62. Shahbazian D, Roux PP, Mieulet V, Cohen MS, Raught B, Taunton J, et al. The mTOR/PI3K and MAPK pathways converge on eIF4B to control its phosphorylation and activity. EMBO J. 2006;25(12):2781-91.
63. Rosario FJ, Powell TL, Gupta MB, Cox L, Jansson T. mTORC1 Transcriptional Regulation of Ribosome Subunits, Protein Synthesis, and Molecular Transport in Primary Human Trophoblast Cells. Frontiers in Cell and Developmental Biology. 2020;8.
64. Chau KF, Shannon ML, Fame RM, Fonseca E, Mullan H, Johnson MB, et al. Downregulation of ribosome biogenesis during early forebrain development. eLife. 2018;7:e36998.
65. Grönberg C, Nilsson J, Wigren M. Recent advances on CD4+ T cells in atherosclerosis and its implications for therapy. European Journal of Pharmacology. 2017;816:58-66.
66. Zhao Y, Qian Y, Sun Z, Shen X, Cai Y, Li L, et al. Role of PI3K in the Progression and Regression of Atherosclerosis. Frontiers in Pharmacology. 2021;12.
67. Flynn MC, Pernes G, Lee MKS, Nagareddy PR, Murphy AJ. Monocytes, Macrophages, and Metabolic Disease in Atherosclerosis. Front Pharmacol. 2019;10:666.
68. Gupta Rajat M, Lee-Kim Vivian S, Libby P. The March of Monocytes in Atherosclerosis. Circ Res. 2020;126(10):1324-6.
69. Ley K, Miller YI, Hedrick CC. Monocyte and macrophage dynamics during atherogenesis. Arterioscler Thromb Vasc Biol. 2011;31(7):1506-16.
70. Llodrá J, Angeli V, Liu J, Trogan E, Fisher EA, Randolph GJ. Emigration of monocyte-derived cells from atherosclerotic lesions characterizes regressive, but not progressive, plaques. Proceedings of the National Academy of Sciences of the United States of America. 2004;101(32):11779-84.
71. Merino A, Buendia P, Martin-Malo A, Aljama P, Ramirez R, Carracedo J. Senescent CD14+CD16+ monocytes exhibit proinflammatory and proatherosclerotic activity. J Immunol. 2011;186(3):1809-15.
72. Ong S-M, Hadadi E, Dang T-M, Yeap W-H, Tan CT-Y, Ng T-P, et al. The pro-inflammatory phenotype of the human non-classical monocyte subset is attributed to senescence. Cell Death & Disease. 2018;9(3):266.
73. Rafieian-Kopaei M, Setorki M, Doudi M, Baradaran A, Nasri H. Atherosclerosis: process, indicators, risk factors and new hopes. Int J Prev Med. 2014;5(8):927-46.
74. Randolph GJ. The fate of monocytes in atherosclerosis. J Thromb Haemost. 2009;7 Suppl 1(Suppl 1):28-30.
75. Wilson HM. Macrophages heterogeneity in atherosclerosis - implications for therapy. J Cell Mol Med. 2010;14(8):2055-65.
76. Woollard KJ, Geissmann F. Monocytes in atherosclerosis: subsets and functions. Nature reviews Cardiology. 2010;7(2):77-86.
77. Gerhardt T, Ley K. Monocyte trafficking across the vessel wall. Cardiovasc Res. 2015;107(3):321-30.
78. Taylor JP, Tse HM. The role of NADPH oxidases in infectious and inflammatory diseases. Redox Biology. 2021;48:102159.
79. Zhang J, Li H, Wu Q, Chen Y, Deng Y, Yang Z, et al. Tumoral NOX4 recruits M2 tumor-associated macrophages via ROS/PI3K signaling-dependent various cytokine production to promote NSCLC growth. Redox Biology. 2019;22:101116.

80. Hao JJ, Liu Y, Kruhlak M, Debell KE, Rellahan BL, Shaw S. Phospholipase C-mediated hydrolysis of PIP2 releases ERM proteins from lymphocyte membrane. J Cell Biol. 2009;184(3):451-62.
81. Gupta N, Wollscheid B, Watts JD, Scheer B, Aebersold R, DeFranco AL. Quantitative proteomic analysis of B cell lipid rafts reveals that ezrin regulates antigen receptor-mediated lipid raft dynamics. Nat Immunol. 2006;7(6):625-33.
82. Parameswaran N, Matsui K, Gupta N. Conformational switching in ezrin regulates morphological and cytoskeletal changes required for B cell chemotaxis. J Immunol. 2011;186(7):4088-97.
83. Bradley JR. TNF-mediated inflammatory disease. The Journal of Pathology. 2008;214(2):149-60.
84. Mehta AK, Gracias DT, Croft M. TNF activity and T cells. Cytokine. 2018;101:14-8.
85. Jones SJ, Ledgerwood EC, Prins JB, Galbraith J, Johnson DR, Pober JS, et al. TNF recruits TRADD to the plasma membrane but not the trans-Golgi network, the principal subcellular location of TNF-R1. J Immunol. 1999;162(2):1042-8.
86. Zhang Q, Cui F, Fang L, Hong J, Zheng B, Zhang JZ. TNF-α impairs differentiation and function of TGF-β-induced Treg cells in autoimmune diseases through Akt and Smad3 signaling pathway. J Mol Cell Biol. 2013;5(2):85-98.
87. Azari BM, Marmur JD, Salifu MO, Ehrlich YH, Kornecki E, Babinska A. Transcription and translation of human F11R gene are required for an initial step of atherogenesis induced by inflammatory cytokines. Journal of Translational Medicine. 2011;9(1):98.
88. Theilmeier G, Michiels C, Spaepen E, Vreys I, Collen D, Vermylen J, et al. Endothelial von Willebrand factor recruits platelets to atherosclerosis-prone sites in response to hypercholesterolemia. Blood. 2002;99(12):4486-93.
89. Massberg S, Brand K, Grüner S, Page S, Müller E, Müller I, et al. A critical role of platelet adhesion in the initiation of atherosclerotic lesion formation. J Exp Med. 2002;196(7):887-96.
90. Woodfin A, Voisin M-B, Nourshargh S. PECAM-1: A Multi-Functional Molecule in Inflammation and Vascular Biology. Arteriosclerosis, Thrombosis, and Vascular Biology. 2007;27(12):2514-23.
91. Stevens HY, Melchior B, Bell KS, Yun S, Yeh JC, Frangos JA. PECAM-1 is a critical mediator of atherosclerosis. Dis Model Mech. 2008;1(2-3):175-81; discussion 9.
92. Caligiuri G. CD31 as a Therapeutic Target in Atherosclerosis. Circ Res. 2020;126(9):1178-89.
93. Cornwell A, Palli R, Singh MV, Benoodt L, Tyrell A, Abe JI, et al. Molecular characterization of atherosclerosis in HIV positive persons. Sci Rep. 2021;11(1):3232.
94. Saigusa R, Winkels H, Ley K. T cell subsets and functions in atherosclerosis. Nature Reviews Cardiology. 2020;17(7):387-401.
95. Reed JC, Preston-Hurlburt P, Philbrick W, Betancur G, Korah M, Lucas C, et al. The receptor for advanced glycation endproducts (RAGE) modulates T cell signaling. PLOS ONE. 2020;15(9):e0236921.
96. Schäfer S, Zernecke A. CD8(+) T Cells in Atherosclerosis. Cells. 2020;10(1).
97. van Duijn J, Kritikou E, Benne N, van der Heijden T, van Puijvelde GH, Kroner MJ, et al. CD8+ T-cells contribute to lesion stabilization in advanced atherosclerosis by limiting macrophage content and CD4+ T-cell responses. Cardiovasc Res. 2019;115(4):729-38.
98. van Duijn J, Kuiper J, Slutter B. The many faces of CD8+ T cells in atherosclerosis. Current opinion in lipidology. 2018;29(5):411-6.
99. Cochain C, Zernecke A. Protective and pathogenic roles of CD8(+) T cells in atherosclerosis. Basic research in cardiology. 2016;111(6):71.
100. Castilho JL, Shepherd BE, Koethe J, Turner M, Bebawy S, Logan J, et al. CD4+/CD8+ ratio, age, and risk of serious noncommunicable diseases in HIV-infected adults on antiretroviral therapy. AIDS (London, England). 2016;30(6):899-908.
101. Flynn MC, Pernes G, Lee MKS, Nagareddy PR, Murphy AJ. Monocytes, Macrophages, and Metabolic Disease in Atherosclerosis. Frontiers in Pharmacology. 2019;10(666).
102. Cochain C, Zernecke A. Macrophages and immune cells in atherosclerosis: recent advances and novel concepts. Basic research in cardiology. 2015;110(4):34.

103. Shrestha S, Irvin MR, Grunfeld C, Arnett DK. HIV, inflammation, and calcium in atherosclerosis. Arterioscler Thromb Vasc Biol. 2014;34(2):244-50.
104. Crowe SM, Westhorpe CL, Mukhamedova N, Jaworowski A, Sviridov D, Bukrinsky M. The macrophage: the intersection between HIV infection and atherosclerosis. J Leukoc Biol. 2010;87(4):589-98.
105. Bianchi ME, Mezzapelle R. The Chemokine Receptor CXCR4 in Cell Proliferation and Tissue Regeneration. Frontiers in Immunology. 2020;11.
106. Vogl T, Tenbrock K, Ludwig S, Leukert N, Ehrhardt C, van Zoelen MA, et al. Mrp8 and Mrp14 are endogenous activators of Toll-like receptor 4, promoting lethal, endotoxin-induced shock. Nat Med. 2007;13(9):1042-9.
107. Crowe LAN, McLean M, Kitson SM, Melchor EG, Patommel K, Cao HM, et al. S100A8 & S100A9: Alarmin mediated inflammation in tendinopathy. Sci Rep. 2019;9(1):1463.
108. Shalek AK, Satija R, Adiconis X, Gertner RS, Gaublomme JT, Raychowdhury R, et al. Single-cell transcriptomics reveals bimodality in expression and splicing in immune cells. Nature. 2013;498(7453):236-40.
109. Trinh H-C, Kwon Y-K. A novel constrained genetic algorithm-based Boolean network inference method from steady-state gene expression data. Bioinformatics. 2021;37(Supplement_1):i383-i91.
110. Lim CY, Wang H, Woodhouse S, Piterman N, Wernisch L, Fisher J, et al. BTR: training asynchronous Boolean models using single-cell expression data. BMC Bioinformatics. 2016;17(1):355.
111. Egaña-Gorroño L, López-Díez R, Yepuri G, Ramirez LS, Reverdatto S, Gugger PF, et al. Receptor for Advanced Glycation End Products (RAGE) and Mechanisms and Therapeutic Opportunities in Diabetes and Cardiovascular Disease: Insights From Human Subjects and Animal Models. Front Cardiovasc Med. 2020;7:37.
112. Kosmopoulos M, Drekolias D, Zavras PD, Piperi C, Papavassiliou AG. Impact of advanced glycation end products (AGEs) signaling in coronary artery disease. Biochimica et Biophysica Acta (BBA) - Molecular Basis of Disease. 2019;1865(3):611-9.
113. Narumi K, Miyakawa R, Ueda R, Hashimoto H, Yamamoto Y, Yoshida T, et al. Proinflammatory Proteins S100A8/S100A9 Activate NK Cells via Interaction with RAGE. The Journal of Immunology. 2015;194(11):5539-48.
114. Hofmann Bowman MA, Schmidt AM. S100/calgranulins EN-RAGEing the blood vessels: implications for inflammatory responses and atherosclerosis. Am J Cardiovasc Dis. 2011;1(1):92-100.
115. Barlovic DP, Soro-Paavonen A, Jandeleit-Dahm KA. RAGE biology, atherosclerosis and diabetes. Clin Sci (Lond). 2011;121(2):43-55.
116. Yan SF, Ramasamy R, Schmidt AM. The receptor for advanced glycation endproducts (RAGE) and cardiovascular disease. Expert Rev Mol Med. 2009;11:e9.
117. Sparvero LJ, Asafu-Adjei D, Kang R, Tang D, Amin N, Im J, et al. RAGE (Receptor for Advanced Glycation Endproducts), RAGE Ligands, and their role in Cancer and Inflammation. Journal of Translational Medicine. 2009;7(1):17.
118. Nienhuis HL, Westra J, Smit AJ, Limburg PC, Kallenberg CG, Bijl M. AGE and their receptor RAGE in systemic autoimmune diseases: an inflammation propagating factor contributing to accelerated atherosclerosis. Autoimmunity. 2009;42(4):302-4.
119. Jandeleit-Dahm K, Watson A, Soro-Paavonen A. The AGE/RAGE axis in diabetes-accelerated atherosclerosis. Clin Exp Pharmacol Physiol. 2008;35(3):329-34.
120. Li H, Zhang L, Yin D, Zhang Y, Miao J. Targeting Phosphatidylcholine-Specific Phospholipase C for Atherogenesis Therapy. Trends in Cardiovascular Medicine. 2010;20(5):172-6.
121. Zhou Q, Liao JK. Rho kinase: an important mediator of atherosclerosis and vascular disease. Curr Pharm Des. 2009;15(27):3108-15.
122. Hartmann S, Ridley AJ, Lutz S. The Function of Rho-Associated Kinases ROCK1 and ROCK2 in the Pathogenesis of Cardiovascular Disease. Front Pharmacol. 2015;6:276.
123. Cai A, Zhou Y, Li L. Rho-GTPase and Atherosclerosis: Pleiotropic Effects of Statins. J Am Heart Assoc. 2015;4(7).

124. Jin SY, Kim EK, Ha JM, Lee DH, Kim JS, Kim IY, et al. Insulin regulates monocyte trans-endothelial migration through surface expression of macrophage-1 antigen. Biochim Biophys Acta. 2014;1842(9):1539-48.
125. Zhou Y, Wang Y, Qiao S, Yin L. Effects of Apelin on Cardiovascular Aging. Frontiers in Physiology. 2017;8.
126. Pitkin SL, Maguire JJ, Kuc RE, Davenport AP. Modulation of the apelin/APJ system in heart failure and atherosclerosis in man. British Journal of Pharmacology. 2010;160(7):1785-95.
127. Ahrens TD, Bang-Christensen SR, Jørgensen AM, Løppke C, Spliid CB, Sand NT, et al. The Role of Proteoglycans in Cancer Metastasis and Circulating Tumor Cell Analysis. Front Cell Dev Biol. 2020;8:749.
128. Edwards IJ. Proteoglycans in prostate cancer. Nat Rev Urol. 2012;9(4):196-206.
129. Aberle H. Axon Guidance and Collective Cell Migration by Substrate-Derived Attractants. Front Mol Neurosci. 2019;12:148.
130. Russell SA, Bashaw GJ. Axon guidance pathways and the control of gene expression. Dev Dyn. 2018;247(4):571-80.
131. Tavares LP, Negreiros-Lima GL, Lima KM, E Silva PMR, Pinho V, Teixeira MM, et al. Blame the signaling: Role of cAMP for the resolution of inflammation. Pharmacological Research. 2020;159:105030.
132. Huang S. Reprogramming cell fates: reconciling rarity with robustness. BioEssays : news and reviews in molecular, cellular and developmental biology. 2009;31(5):546-60.
133. Huang S, Eichler G, Bar-Yam Y, Ingber DE. Cell fates as high-dimensional attractor states of a complex gene regulatory network. Physical review letters. 2005;94(12):128701.
134. Huang S, Ernberg I, Kauffman S. Cancer attractors: a systems view of tumors from a gene network dynamics and developmental perspective. Seminars in cell & developmental biology. 2009;20(7):869-76.
135. Taherian Fard A, Ragan MA. Modeling the Attractor Landscape of Disease Progression: a Network-Based Approach. Front Genet. 2017;8:48.
136. Uthamacumaran A. A review of dynamical systems approaches for the detection of chaotic attractors in cancer networks. Patterns (N Y). 2021;2(4):100226.
137. Trapnell C. Defining cell types and states with single-cell genomics. Genome Res. 2015;25(10):1491-8.
138. Munsky B, Neuert G, van Oudenaarden A. Using gene expression noise to understand gene regulation. Science (New York, NY). 2012;336(6078):183-7.
139. Liu S, Trapnell C. Single-cell transcriptome sequencing: recent advances and remaining challenges. F1000Research. 2016;5:F1000 Faculty Rev-182.
140. Tsai S, Clemente-Casares X, Zhou AC, Lei H, Ahn JJ, Chan YT, et al. Insulin Receptor-Mediated Stimulation Boosts T Cell Immunity during Inflammation and Infection. Cell Metab. 2018;28(6):922-34.e4.
141. Arasanz H, Gato-Cañas M, Zuazo M, Ibañez-Vea M, Breckpot K, Kochan G, et al. PD1 signal transduction pathways in T cells. Oncotarget. 2017;8(31):51936-45.
142. Zhao Y, Shao Q, Peng G. Exhaustion and senescence: two crucial dysfunctional states of T cells in the tumor microenvironment. Cellular & Molecular Immunology. 2020;17(1):27-35.
143. Yi H-S, Kim SY, Kim JT, Lee Y-S, Moon JS, Kim M, et al. T-cell senescence contributes to abnormal glucose homeostasis in humans and mice. Cell Death & Disease. 2019;10(3):249.
144. McLaughlin T, Liu L-F, Lamendola C, Shen L, Morton J, Rivas H, et al. T-cell profile in adipose tissue is associated with insulin resistance and systemic inflammation in humans. Arteriosclerosis, thrombosis, and vascular biology. 2014;34(12):2637-43.
145. Singh MV, Kotla S, Le N-T, Ae Ko K, Heo K-S, Wang Y, et al. Senescent Phenotype Induced by p90RSK-NRF2 Signaling Sensitizes Monocytes and Macrophages to Oxidative Stress in HIV-Positive Individuals. Circulation. 2019;139(9):1199-216.

146. Rattan V, Shen Y, Sultana C, Kumar D, Kalra VK. Glucose-induced transmigration of monocytes is linked to phosphorylation of PECAM-1 in cultured endothelial cells. American Journal of Physiology-Endocrinology and Metabolism. 1996;271(4):E711-E7.

147. Okouchi M, Okayama N, Imai S, Omi H, Shimizu M, Fukutomi T, et al. High insulin enhances neutrophil transendothelial migration through increasing surface expression of platelet endothelial cell adhesion molecule-1 via activation of mitogen activated protein kinase. Diabetologia. 2002;45(10):1449-56.

148. Kharchenko PV, Silberstein L, Scadden DT. Bayesian approach to single-cell differential expression analysis. Nature methods. 2014;11(7):740-2.

149. Brorson IS, Eriksson A, Leikfoss IS, Celius EG, Berg-Hansen P, Barcellos LF, et al. No differential gene expression for CD4(+) T cells of MS patients and healthy controls. Mult Scler J Exp Transl Clin. 2019;5(2):2055217319856903-.

Supplementary Material

1. **Supplementary File 1:**
    - **Filename:** supplementary_file_1.pdf
    - **Description:** Contains Supplementary Figures 1 – 6 and corresponding captions.
2. **Supplementary Table 1:**
    - Filename: *supplementary_table_1.txt*
    - **Description of Supplementary Table 1:** Cluster markers for each subpopulation identified in PBMCs derived from AS+ and AS- PLWH are listed in the file "*supplementary_table_1.csv*". Cluster markers were identified using methods implemented in the Seurat R package, as described in the methods.
3. **Supplementary Table 2:**
    - Filename: supplementary_table_2.xlsx
    - Description of supplementary table 2: supplementary_table_2 contains 2 worksheets, "DE genes in AS+ vs AS-" and "enrichr_kegg". "DE genes in AS+ vs AS-" contains a table of genes differentially expressed between cells derived from AS+ and AS- PLWH for each subpopulation in the HIV/AS dataset. The sheet "enrichr_kegg" contains a table of KEGG gene sets enriched (identified using the enrichr R package) in the DE genes from "DE genes in AS+ vs AS-".
4. **Supplementary Table 3:**
    - **Filename:** *supplementary_table_3.txt*
    - **Description of Supplementary Table 3:** scBONITA infers biologically meaningful dysregulated pathways for subpopulations of PBMCs derived from AS+ and AS- PLWH in the HIVAS/HIVAS- contrast. The table of dysregulated pathways identified by scBONITA in the HIV+/AS+ - HIV+/AS- contrast in all cell clusters is presented in the CSV file titled "*supplementary_table_3.txt*".

5. **Supplementary Table 4**
    - **Filename:** *supplementary_table_4.txt*
    - **Description:** Pearson correlation coefficients between importance scores for networks trained on subpopulations of PBMCs from the Kazer et al dataset and trained on the corresponding subpopulations from the HIV/AS dataset. All p values are < 0.01.
6. **Supplementary Table 5**
    - **Filename:** *supplementary_table_5.txt*
    - **Description:** scBONITA infers biologically meaningful dysregulated pathways for subpopulations of PBMCs derived from HIV- subjects and subjects after 1 year of HIV infection (Kazer et al). The CSV file *supplementary_table_5.txt* lists the dysregulated pathways and p-values from scBONITA for every subpopulation.
7. **Supplementary Table 6**
    - **Filename:** *supplementary_table_6.txt*
    - **Description:** Comparison of dysregulated pathways, as identified by scBONITA, between subpopulations of PBMCs derived from HIV- subjects and subjects after 1 year of HIV infection (Kazer et al) and subpopulations of PBMCs derived from HIV+ subjects with and without atherosclerosis. The file *supplementary_table_6.txt* lists the dysregulated pathways for subpopulations from the Kazer et al dataset and the corresponding subpopulations from the HIV/AS dataset, along with the intersections between the pathways dysregulated in the two contrasts. We speculate that intersecting pathways and the pathways dysregulated in the HIV/AS contrast are driven by HIV-associated inflammatory processes. Similarly, pathways that are dysregulated only in the HIV-/HIV+ contrast are assumed to be driven by the immediate antiviral response to HIV infection.

Figures

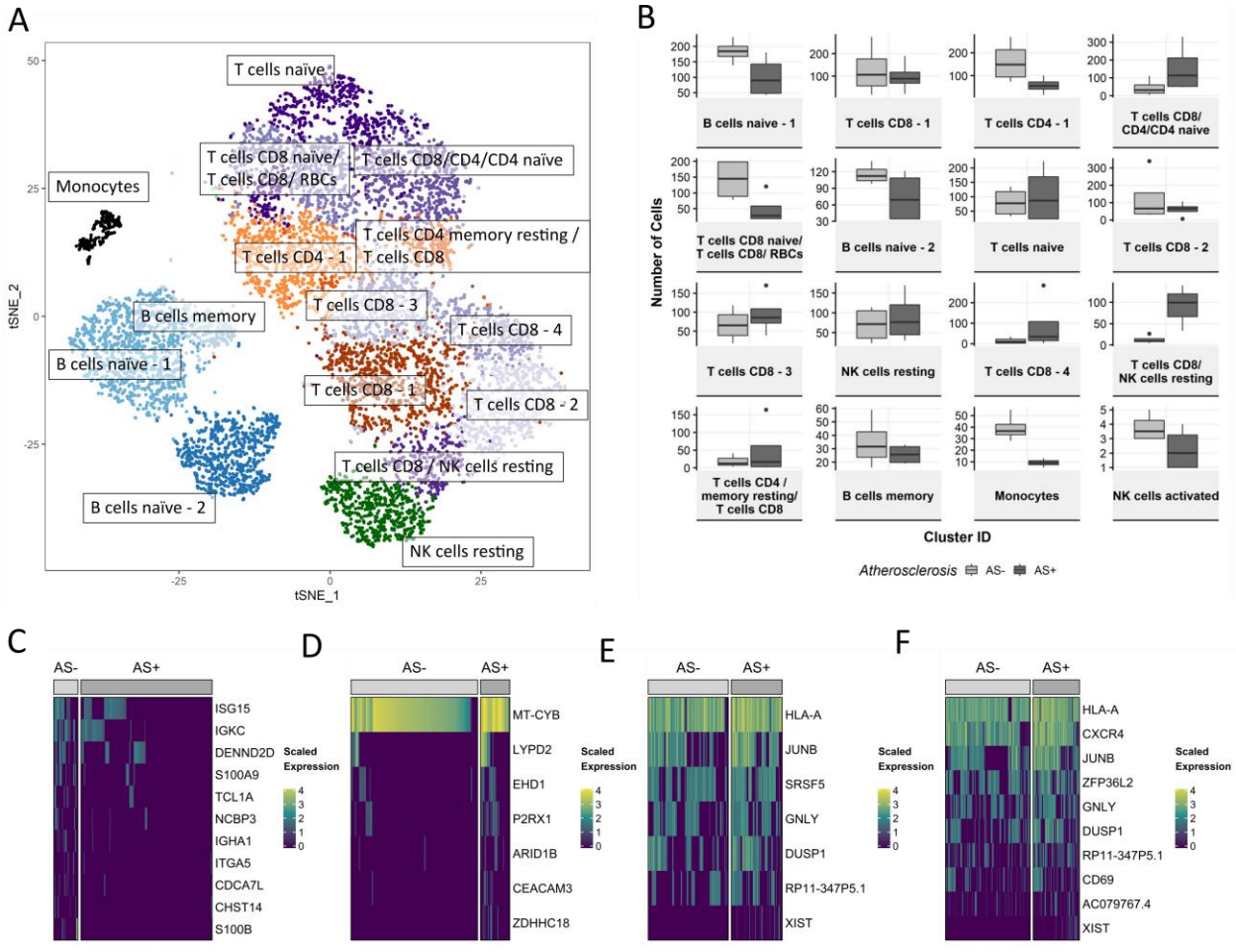

Figure 1: Characterization of PBMC subpopulations in people living with HIV (PLWH) with (AS+) or without atherosclerosis (AS-) (A) t-SNE projection of 16 transcriptionally distinct cell subpopulations, shown in distinct colors. Cell clusters are characterized and labeled based on the expression of canonical markers, using CIBERSORT. (B) Subpopulation-level differences between AS+ and AS- PLWH are identified using a t-test. Panels C - F show the expression of genes that are differentially expressed (DE) between cells derived from AS+ and AS- subjects. DE genes were identified using the Wilcoxon test (Bonferroni-adjusted p-value < 0.1, absolute log2 fold change > 0.3.) DE genes between AS+ and AS- cells in (C) CD8 T cells/NK resting cells, (D) monocytes, (E) naïve B cells referred to as "B cells naïve - 2" in panels A and B, and (F) T cells referred to as "T cells CD8/CD4/CD4 naïve" in panels A and B.

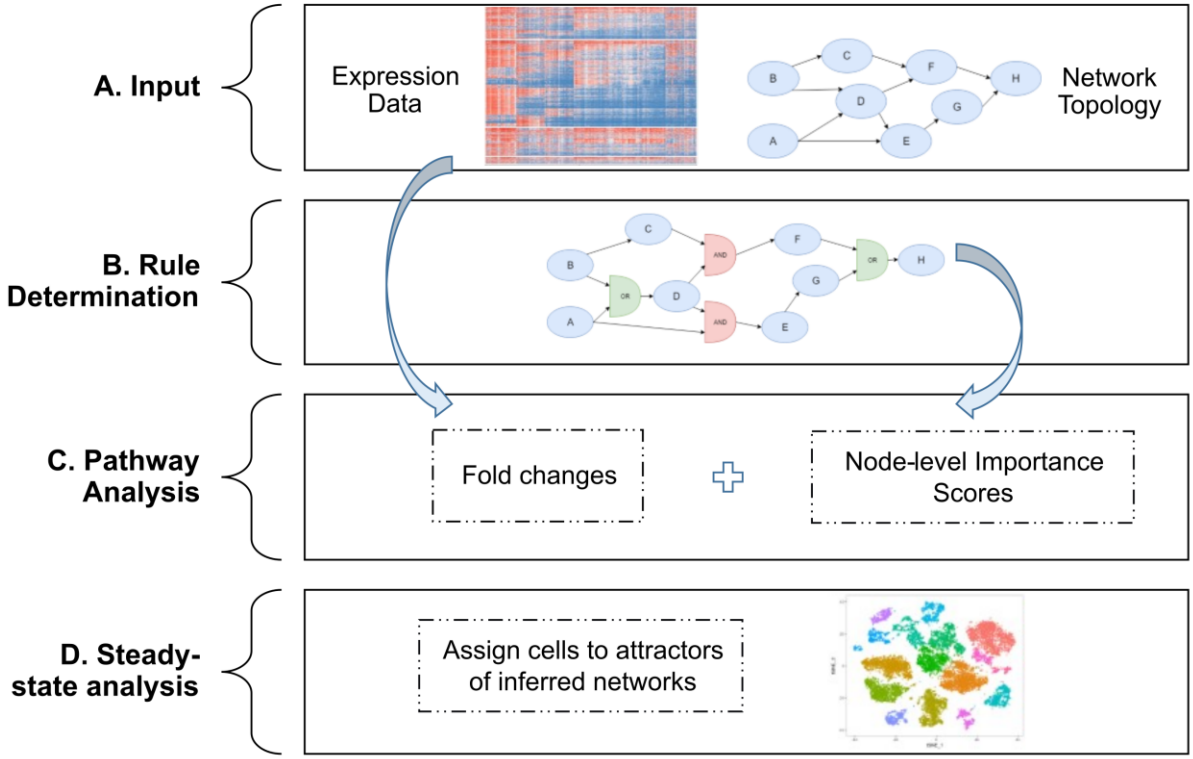

Figure 2: scBONITA pipeline to infer Boolean rules and perform pathway analysis using single cell expression measurements (A) **Input**: scBONITA requires a binarized single-cell RNA-seq dataset as a text file, and a prior knowledge network (PKN) describing the activating or inhibitory relationships between genes (B) **Rule determination:** scBONITA infers logic rules that describe the regulatory relationships between nodes in the PKN by a global search followed by node-level rule refinement (C) **Pathway analysis:** scBONITA calculates a gene importance score calculated by simulating network perturbations with inferred rules and combines these scores with fold-changes from scRNA-seq to identify dysregulated pathways in a specified contrast (D) **Steady-state analysis**: scBONITA simulates networks using learned rules to identify steady states which correspond to observed cellular states.

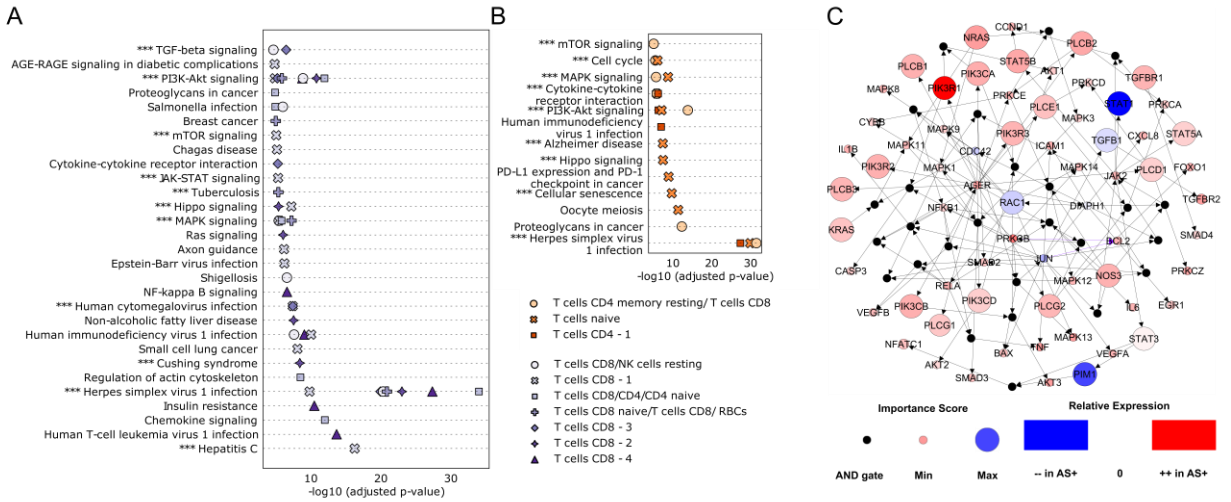

1235

1236 **Figure 3:** scBONITA identifies dysregulated pathways in T cells derived from AS+ and AS- PLWH. (A)
1237 Pathways (y-axis) dysregulated in the AS+ vs AS- contrast in PLWH in clusters of CD8+ T cells. Clusters
1238 are differentiated by point shape, as shown in the legend. Pathways that have Bonferroni-corrected p-
1239 value < 0.01 (x-axis) and a reduced ERS (see Methods for details) are shown. Pathways labeled with
1240 "***" were also significantly dysregulated between cytotoxic T cells derived from HIV- subjects and
1241 subjects after 1 year of HIV infection (36) (B) (Pathways (y-axis) dysregulated in the AS+ vs AS-
1242 contrast in PLWH in clusters of CD4+ T cells and naïve T cells. Clusters are differentiated by point
1243 shape, as shown in the legend. Pathways that have Bonferroni-corrected p-value < 0.01 (x-axis) and a
1244 reduced ERS (see Methods for details) are shown. Pathways labeled with "***" were also significantly
1245 dysregulated between T cells derived from HIV- subjects and subjects after 1 year of HIV infection (36)
1246 (C) Network representation of the AGE-RAGE signaling pathway (Bonferroni-corrected p-value < 0.01)
1247 in a cluster of CD8+ T cells referred to as CD8 T cells -1 in Figure 1A. Small black intermediate nodes
1248 indicate that the downstream nodes are controlled by an AND function of the upstream nodes. The size of
1249 nodes corresponding to genes is proportional to their importance score calculated by scBONITA. Nodes
1250 are colored according to the magnitude of their fold change between the HIV+AS+ and HIV+AS- groups.
1251 Violet edges indicate inhibition edges and black edges indicate activation edges.

1252

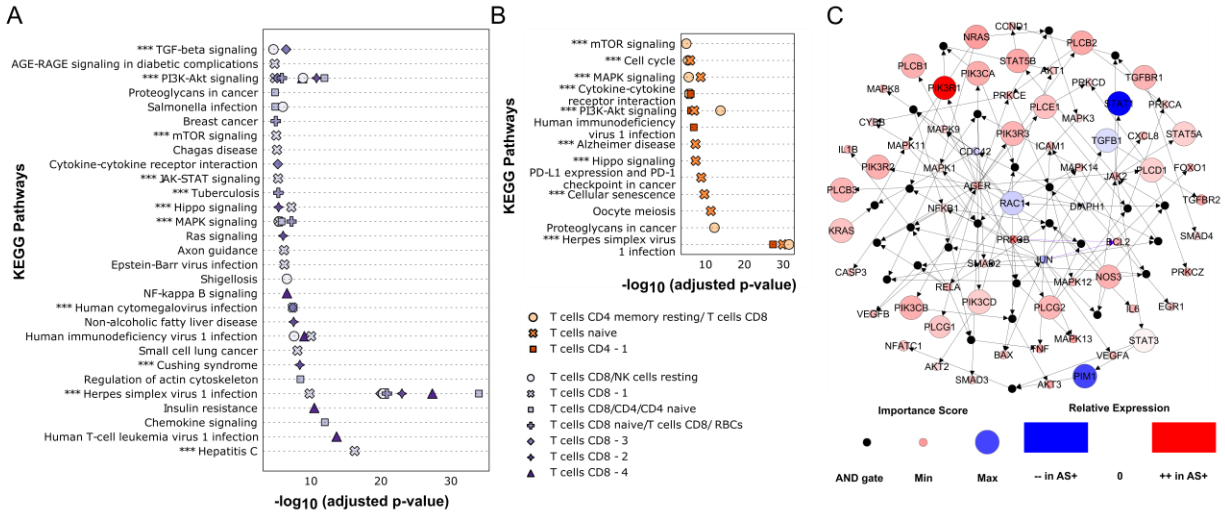

Figure 4: scBONITA identifies dysregulated pathways in monocytes derived from AS+ and AS- PLWH: (A) Pathways (y-axis) dysregulated in the AS+ vs AS- contrast in monocytes derived from PLWH. Only pathways that have Bonferroni-corrected p-value < 0.01 (x-axis) and which have a reduced ERS (see Methods for details) are shown. Pathways labeled with "***" were also significantly dysregulated in monocytes after one year of HIV infection (36) (B) Network representation of the leukocyte transendothelial migration pathway. Small black intermediate nodes indicate that the downstream nodes are controlled by an AND function of the upstream nodes. The size of nodes corresponding to genes is proportional to their importance score as calculated by scBONITA. Nodes are colored according to the magnitude of their fold change between the HIV+AS+ and HIV+AS- groups. Violet edges indicate inhibition edges and black edges indicate activation edges.

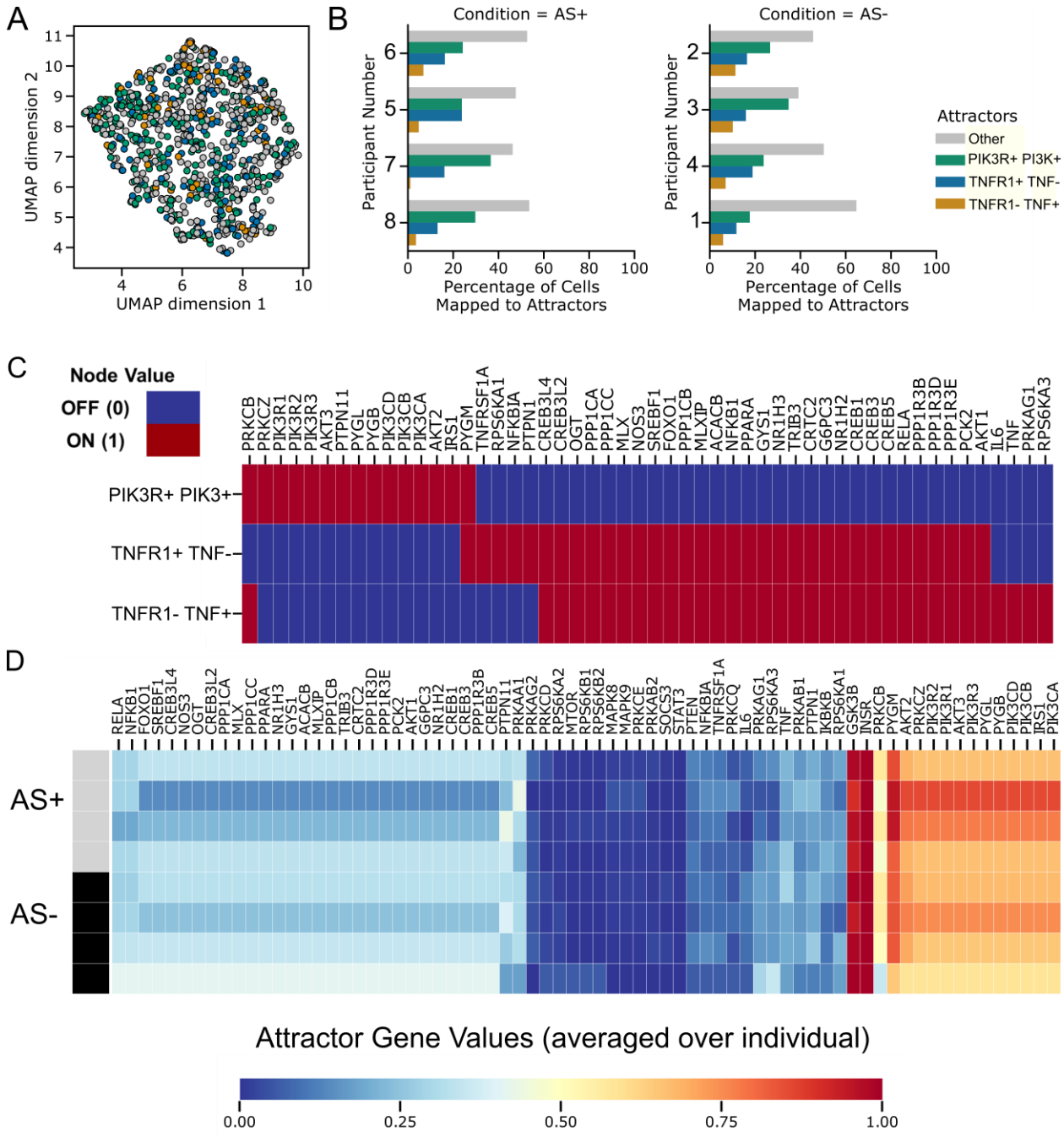

Figure 5: CD8+ T cell states with respect to the insulin resistance pathway identified by attractor analysis with scBONITA. (A) UMAP representation of a cluster of CD8+ T cells (CD8+ T cells – 1 in Figure 1A) colored by the attractor to which they are assigned, based on their similarity. The three dominant states (PI3KR+ PI3K+, TNFR1+TNF- and TNFR1-TNF+ attractors) are represented by green, blue and orange.

1271 All other attractors are collectively labeled in grey. (B) Percentages of CD8+ T cells derived from each
1272 subject, mapping to the three dominant and all other attractors. (C) Gene activity (ON- red, OFF- light
1273 blue) in the three dominant attractors. Only genes that are different between these states are shown. (D)
1274 Attractor gene values ranging from 0 (blue) to 1 (red) averaged for each individual subject. The top bar
1275 indicates AS+ (grey) and AS- (black) subjects.
1276

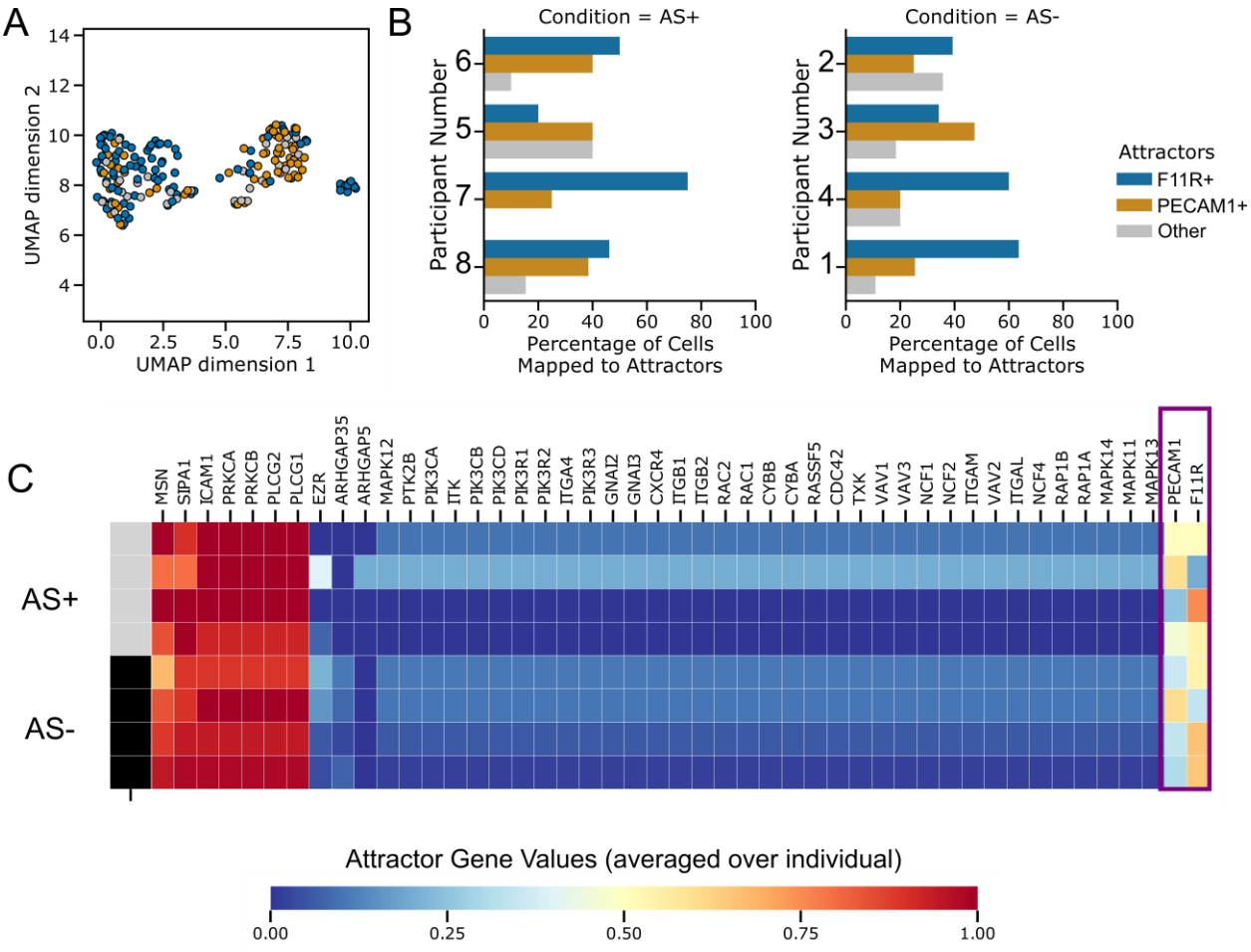

Figure 6: Monocyte states with respect to the leukocyte transendothelial migration pathway identified by attractor analysis with scBONITA. (A) UMAP representation of the cluster of monocytes colored by the attractor to which they are assigned, based on their similarity. The two dominant modes (F11R+ and PECAM+ attractors) are represented by blue and orange. All other attractors are collectively labeled in grey. (B) Percentages of monocytes derived from each subject, mapping to the two dominant attractors and all other attractors for the leukocyte transendothelial migration pathway. (C) Attractor gene values for the for the leukocyte transendothelial migration pathway trained on monocytes, ranging from 0 (blue) to 1 (red), averaged for each individual subjects. The top bar indicates AS+ (grey) and AS- (black) subjects. The genes that differ between the two dominant attractors F11R+ and PECAM+ are highlighted by a violet box.

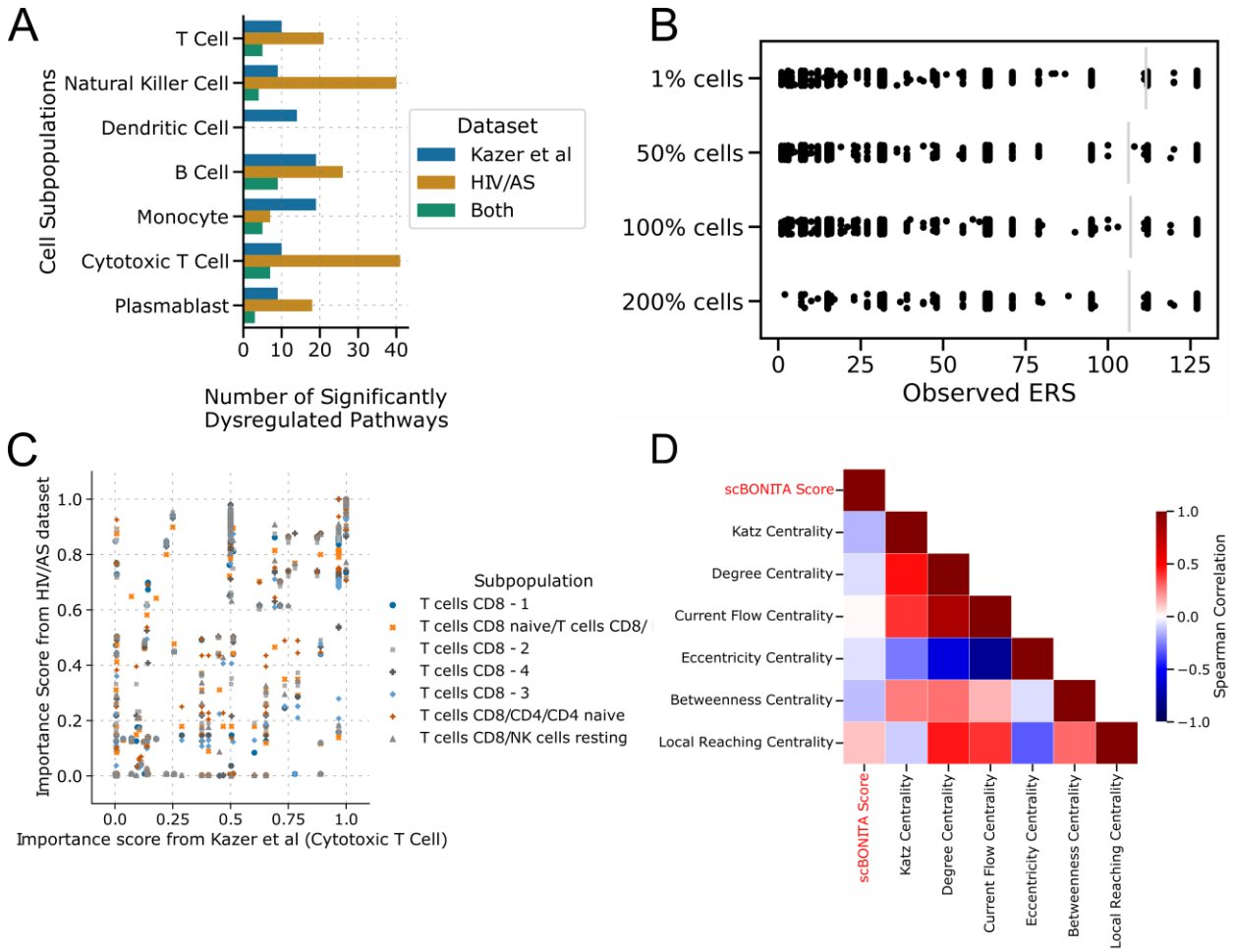

Figure 7: Performance of scBONITA rule determination. (A) The number of pathways identified as significantly dysregulated (Bonferroni-adjusted p value < 0.05) one year upon HIV infection(36), between AS+ and AS- PLWH, and the intersections between these sets. Subpopulations from the two datasets were matched as shown in Supplementary Table 5. (B) Effects of number of cells on the ERS size evaluated by downsampling and augmentation using the largest cluster ("B cells naïve – 1") from the HIV/AS dataset (C) Relation between importance scores in 130 KEGG networks evaluated using CD8+ T cells from AS+ and AS- PLWH and from persons before and one year after HIV infection (36). (D) Spearman correlations ($p < 0.01$ for all comparisons) between scBONITA's node importance score (labeled as 'scBONITA score') and 6 measures of node centrality (along x and y axis). Correlation coefficients are depicted by colors ranging from blue (-1) to red (+1).